GMD-2016-233 Final Author Responses

Dear David,

Please find our responses to the editor and referee comments compiled below, together with the corresponding manuscript changes. The second part of the document includes the revised manuscript with all corresponding changes marked in yellow.

In addition to the referee comments, we found a couple of instances where we weren't clear enough about the projection time periods. Related edits have also been marked in yellow. We have also corrected a few grammatical errors and typos. Those are not highlighted in the marked-up in the manuscript.

We hope that our responses and edits together with the provision of the MAGICC source code package address all issues raised by the editor and the referees. Please let us know if you request any further revisions.

Best regards,
Alexander, for the author team

Executive Editor

Received and published: 24 February 2016

Editor General Comment (EC1.00): *Dear authors, in my role as Executive editor of GMD, I would like to bring to your attention our Editorial version 1.1. This highlights some requirements of papers published in GMD, which is also available on the GMD website in the 'Manuscript Types' section. In particular, please note that for your paper, the following requirement has not been met in the Discussions paper: "The main paper must give the model name and version number (or other unique identifier) in the title." Please add a version number for MAGICC in the title upon your revised submission to GMD. Additionally, please note that the Code and Data Availability Section is not a numbered Section. Yours, Astrid Kerkweg*

Author Response (AR0.00):

Thank you for pointing us to the necessary title revision. Previous MAGICC model versions provided sea level estimates based on varying sea level components (Wigley and Raper 2005, Wigley 1995, Wigley and Raper 1987, Wigley and Raper 1992). These older developments can be seen as MAGICC sea level model versions 1.0, 1.1, 1.2, 1.3 etc. Here, we here present a new, fully revised MAGICC sea level model which will be also part of the coming MAGICC model version release. Thus, we suggest the following title: "Synthesizing long-term sea level rise projections – the MAGICC sea level model v2.0"

Anonymous Referee #1

Received and published: 10 February 2017

Referee #1 General Comment (RC1.00): *In this paper, the authors describe the first version of the MAGICC sea level model, a set of sea-level emulators linked to versions 6 and 7 of the MAGICC climate model. They provide a clear description of the algorithms for the different sea-level components and of the model calibration. Accordingly, I believe the paper is worth publishing and have only minor comments*

regarding the paper itself. I suggest the authors add some discussion placing the MAGICC sea level model in the context of other similar tools, such as the BRICK model, also currently in review at GMD (http://dx.doi.org/10.5194/gmd-2016-303). A comparison of the model results to that of other simple sea-level models (e.g., Kopp et al., 2016, and Mengel et al., 2016) under similar forcing would be helpful – prima facie, the projections for 2100 seem to align well with these simpler models.

Author Response (AR1.00): We would like to thank the referee for reviewing this manuscript and are encouraged by the positive feedback and the overall recommendation to publish the work with minor revisions. We have extended the discussion on alternative sea level modeling approaches and included hindcast information with comparison datasets, as also requested by referee #2 (Figure A.2). Unfortunately, we find it hard to compare our results directly to the BRICK model, because we could not find any suitable sea level projection time series in the BRICK discussion paper. However, we very much support the efforts by the author team to provide a simple and transparent sea level model framework and have now referenced the discussion paper in our introduction (p.3 l.5). It is encouraging that also other simple model frameworks are in line with recent comprehensive reference assessments. Our key objective was to develop a simple but comprehensive sea level model that emulates the process-based reference data from the Fifth Assessment Report of the IPCC. Consequently, mainly IPCC datasets are used for comparison in the manuscript. Please note that we discovered a bug in the MAGICC routine to prescribe annual mean surface air temperature as well as a problem with the Greenland SID functional form, while carrying out additional checks of the calibration routines after the submission of the manuscript. Also, one specific CMIP5 model input had to be removed due to quality issues with the reference data (BCC-CSM1.1M). All issues have been resolved. The revised prescribed temperature routine required the re-calibration of all sea level model components, with all figures now showing the revised sea level model results. The updated optimal parameter sets are provided in the corresponding Tables. For the Greenland SID parameterisation, the calibrated constant was removed, because it prohibited the reproduction of lower bound projections (see revised Equation 6). In addition, the routine was adapted to allow for hindcasts without depleting the maximum outlet glacier volume, which was determined based on the year 2000. The code repository has been updated to account for these changes. All revised and additional Figures as well as one additional Appendix Table are provided at the end of this document.

RC1.01: *Line 28: I believe the citation here should be to Levermann et al. (2014), not Levermann et al. (2013).*

AR1.01: Well spotted, thank you! The citation is updated.

RC1.02: *Line 30: Note that an early semiempirical model was introduced by Gornitz et al. (1982) twenty five years earlier. Gornitz, V., S. Lebedeff, and J. Hansen, 1982: Global sea level trend in the past century. Science, 215, 1611–1614, doi:10.1126/science.215.4540.1611.*

AR1.02: Thank you for this correct remark. We have revised the text accordingly. The passage on p.2 l.30 now reads: "In the 1980s, first Semi-Empirical Models (SEMs), which estimate global sea level changes based on the evolution of global mean temperature, were introduced together with early attempts to model thermal expansion based on simplified ocean processes (Gornitz, Lebedeff and Hansen 1982). Generally, SEMs establish statistical relationships between observed/reconstructed global mean temperature or radiative forcing changes and observed/reconstructed global mean sea level changes. Assuming that such relationships stay the same for the future, they are used to estimate future SLR from projected global temperature/forcing changes (Jevrejeva, Moore and Grinsted 2010, Kopp et al. 2016, Rahmstorf 2007, Vermeer and Rahmstorf 2009). As such, these SEMs do not calculate sea level by resolving the underlying physical processes."

RC1.03: *I also note that the code for the sea level model, while available at the gitlab link provided, does not run without the MAGICC model, for which code is not available. I further note that GMD policy states: "If the authors cannot or do not wish to make the code and/or data public (e.g. copyright or licensing restrictions), the reasons must be clearly stated. Note that, for the purpose of the review, the code and/or data must still be made available to the editor. Access must also be granted to the reviewers whilst preserving their anonymity, if this is legally possible." I am not sure whether the current code availability – dependent upon code that was not available for the review process, and for whose non-availability no explanation was provided – satisfies this policy.*

AR1.03: We acknowledge that the parent MAGICC model is needed to fully reproduce results with the MAGICC sea level model and regret not providing the source code and a test example with the first version of this manuscript. In order to facilitate the review of the sea level model implementation and to fully support the GMD policies for reproducibility, we have now provided a minimum MAGICC model setup including source code to the editor for distribution to the referees. The sea level model presented in this manuscript is available as open source code on a dedicated gitlab repository, in accordance with the GMD code and data policies. Please see Meinshausen, Raper and Wigley (2011a) and Meinshausen, Wigley and Raper (2011c) for a detailed description of the parent model. MAGICC itself has not been designed as an open-source model, as its initial development and application go back three decades to a time when the open source concept wasn't well established in the scientific community. The source code for MAGICC model version 6 is available under a license agreement on request. Unfortunately, we did not make this clear in the documentation on the digital repository. This has been corrected. We hope that these efforts address the concerns voiced by the referees and allow us to provide a first MAGICC model component on an open-source platform.

Anonymous Referee #2

Received and published: 24 February 2017

Referee #2 General Comment (RC2.00): *The ms tackles an important and nontrivial point and makes several new contributions. The authors are to be applauded for the efforts and providing the new insights. Alas, the current ms suffers from several (in my view severe, but pretty easy to fix) shortcomings that need to be mitigated to enable a careful review and to hopefully (and eventually) rise to the level of quality one expects from papers in GMD. These specific points are discussed below. The ms requires in my view a careful and responsive revision and re-review. I would be happy to look at this ms again.*

Author Response (AR2.00): We thank the referee for this thorough review leading to numerous revisions and additions, which, in our eyes, have substantially improved the manuscript. We regret not having spent more time on the topic of code availability before the initial submission. We hope that our response and the provision of the MAGICC source code address the issues raised by the referee. Please note, that all revised and additional Figures as well as one additional Appendix Table are provided at the end of this document for your convenience.

Referee #2 Comment 1(RC2.01): *The ms does, in my view, not follow the data and code policy of GMD. As a reminder, here is the link describing the policy: GMD code and data policy. These rules state: "Preferably, this section should contain the instructions for obtaining the model code and/or data, either from the supplement or from an archive with a digital object identifier (DOI). Suitable repositories can be found at the Registry of Research Data Repositories, e.g. ZENODO for model code. After the paper is accepted, a link to the GMD paper should be added to the metadata of the archive." What is available, as far as I can tell, is code for the sea-level rise model / module. However, it will be extremely tough to reproduce the results in the paper, due to several issues. For example, the interface to call this module is not well documented, nor are the data used to drive and calibrate the model provided. The web-page the ms links to states: "The*

Fortran code of the model as well as required additional MAGICC input files can be downloaded as a zip-file at the top right of this page. Please note that the MAGICC sea level model is not a stand-alone tool. It is fully integrated into the simple carbon cycle climate model MAGICC and cannot be run separately. The MAGICC model is described in Meinshausen et al. (2011). For a compiled MAGICC version including the sea level model, please contact alexander.nauels@climate-enegy-college.org. MAGICC is licensed under a Creative Commons Attribution-NonCommercial-ShareAlike3.0 Unported License". Does this mean that the source code for the model needed to run the sea-level model is not accessible? Why is only a compiled version distributed? Given this situation, I would assign a very low score for reproducibility (see the discussion by Haas in the recent Risk Analysis volume (Risk Analysis, Vol. 36, No. 10, 2016, DOI: 10.1111/risa.12730). Many other studies have abided by the nice standards outlined in GMD and a publication in GMD should clearly abide by these standards. This is a decision for the editor. I cannot carefully review the ms without the ability to see and run all the code and cannot support publication as a peer reviewed study in GMD with the current state of data availability.

AR2.01: We acknowledge the concerns expressed by the referee and regret that we have not clarified the availability of the MAGICC source code earlier. We hope that the following update resolves this issue. In line with the GMD code and data policies, the sea level model presented here is available as open-source code on a transparent and version-controlled repository. Once the manuscript is accepted in its final version, we will also deposit the sea level code on ZENODO with a DOI. We agree that it is challenging to reproduce the sea level model output without the parent model code. The MAGICC model itself is not open-source, which is mainly due to the long model development history. The model was first introduced in the 1980s, a time when the open-source concept wasn't well established in the science community. Subsequent MAGICC developments have all been carried out without the scope and resources to fully migrate the model to an open-source platform. Unfortunately, the authors of this manuscript are not in a position to go open source with the code in its current version. The model source-code is available for interested researchers under a non-commercial license agreement on request, which is now communicated correctly in the repository documentation. A MAGICC model package with the source-code including the sea level model has been provided to the editor for distribution to the referees to ensure transparency and reproducibility of the presented work. The most recent MAGICC model version 6 has been extensively documented in Meinshausen et al. (2011a) and Meinshausen et al. (2011c). Data for the atmospheric and ocean variables used for the model calibration can be downloaded from the CMIP5 archive. The interpolated calibration data for the MAGICC ocean model are available on request. This is now clarified in the code and data section (p.17 l.20). The other sea level components are calibrated with additional published datasets that were received by courtesy of the respective author teams. With the sea level model code openly provided and the full MAGICC model available to the referees as part of this review and for interested peers upon request, we hope that we have addressed the referee's concerns regarding the data and code policy of GMD.

RC2.02: *The ms emulates model runs that are mostly samples of best guesses on choices such as model parameters and structures. This sample is likely missing important uncertainties. Communicating the range of the projections and the discussing "probabilistic uncertainty analyses" (abstract) can lead to unfortunate misunderstandings by the users. This needs to be discussed and the communication made more clear to help the users of this tool and the results to better understand the caveats. There is a nice start towards this goal on the bottom of page 9, but this needs to be made much more clear to the reader (e.g., in the abstract). This potential misunderstanding is the even strengthened in the design of the projections, that uses a "probabilistic MAGICC design" (p. 14). For example, Figure A1 discusses a 66% range. One question the ms should address is how the ranges they present compare to expert assessments (that are cited in the ms).*

AR2.02: The referee is correct in noting that the presented sea level model does not account for deep uncertainties, i.e., uncertainties due to processes that are not yet known or not captured by process-based models. It is not probabilistic in that sense. Rather, we present an approach to reflect key uncertainties for all major SLR drivers based on the process-based projections presented in the Fifth

Assessment Report of the IPCC. Our model is probabilistic in the sense that we combine parameter uncertainties in a way that results in each calibrated parameter set reasonably reproducing the specific reference data. By applying the well-established probabilistic Metropolis-Hastings Markov chain Monte Carlo projection method from Meinshausen et al. (2009), which also underlies, e.g., Meinshausen et al. (2011b), Rogelj, Meinshausen and Knutti (2012), Perrette et al. (2013), Levermann et al. (2014), we can additionally map key climate and carbon-cycle related uncertainties; above all, the range of equilibrium climate sensitivities presented in IPCC's AR5. The MAGICC sea level emulator therefore provides projections that, besides scenario related uncertainties, reflect model uncertainties included in the reference data (i.e. from the CMIP5 ensemble), as well as uncertainties from carbon-cycle responses (Meinshausen et al. 2011a, Friedlingstein et al. 2014) and latest climate sensitivity estimates (Flato et al. 2013). In order to avoid confusion regarding the scope of uncertainties that can be assessed with the presented approach, we have modified the abstract, with the relevant sentence on p.1 l.18 now reading: "The MAGICC sea level model provides a flexible and efficient platform for the analysis of major scenario, model, and climate uncertainties underlying long-term SLR projections". In addition, we have elaborated on the probabilistic method and the comparison of our Antarctic solid ice discharge projections (90% model range now included in the Appendix figures) to the ones presented in DeConto and Pollard (2016). We have revised p.14 l.17 to read: "In order to also provide a sufficiently large number of model runs for 2300, we use 600 historically-constrained parameter sets that have been derived using a probabilistic Metropolis-Hastings Markov chain Monte Carlo method (Meinshausen et al. 2009). This approach has been extended to also reflect carbon-cycle uncertainties (Friedlingstein et al. 2014) and the climate sensitivity range of the latest IPCC assessment (Flato et al. 2013, Rogelj et al. 2012, Rogelj et al. 2014)"; and the section on p.17 l.1 has been updated: "The Antarctic ice sheet response, for example, could be subject to more rapid, non-linear dynamics that are not captured by the emulated process-based projections. Only recently, DeConto and Pollard (2016) have revised potential future Antarctic contributions to global sea level based on indicators from paleoclimatic archives. For RCP8.5, they project 2100 contributions of around 1m from Antarctica alone, with 2300 contributions reaching up to around 10 m. The MAGICC sea level model projections for the Antarctic SID contribution are based on Levermann et al. (2014) and only yield up to around 0.35 m in 2100 and 2.68 m in 2300 for the upper bound of the 90% range. As the more recent research suggests, these estimates may be too low, indicating that the Antarctic contribution to future SLR is subject to additional uncertainties. This illustrates the need to handle long-term SLR projections with care and to note the corresponding methodological caveats; in particular, those surrounding the representation of Antarctic ice-sheet changes."

RC2.03: *The ms makes several broad and somewhat ambiguous claims that need to be updated. For example, the ms states: "This MAGICC sea level model has been designed to emulate the behavior of the latest available process-based sea level projections" (p2). This does seem to be in contrast with the findings of DeConto and Pollard (2016), which the ms cites but in my reading not considers. This also needs to flow into the discussion of ice sheet dynamics on page 13 as well as the summary in the discussion (p. 15).*

AR2.03: We agree with the referee that our statement regarding the selected reference datasets was deceptive. We have revised the corresponding statement on p.2 l.13 to read: "This MAGICC sea level model has been designed to emulate the behavior of process-based sea level projections presented in the IPCC's Fifth Assessment Report (Church et al. 2013a), with thorough calibrations for each major sea level component." The discussion now includes a direct comparison of the MAGICC sea level model results with the findings from DeConto and Pollard (2016). After searching for other instances of using the potentially ambiguous adjective "latest", we have also decided to change the land water related statement in the abstract on p.1 l.15 to read: "The land water storage component replicates recent hydrological modeling results."

RC2.04: *How are "semi-empirical models" (p2) specifically defined? Has there been no use before 2007 (as the ms seems to imply)?*

AR2.04: We now provide more specific details on the design of semi-empirical models and clarify that the semi-empirical concept has been applied well before 2007. The section on p.2 l.30 now reads: "In the 1980s, first Semi-Empirical Models (SEMs), which estimate global sea level changes based on the evolution of global mean temperature, were introduced together with early attempts to model thermal expansion based on simplified ocean processes (Gornitz et al. 1982). Generally, SEMs establish statistical relationships between observed/reconstructed global mean temperature or radiative forcing changes and observed/reconstructed global mean sea level changes. Assuming that such relationships stay the same for the future, they are used to estimate future SLR from projected global temperature/forcing changes (Jevrejeva et al. 2010, Kopp et al. 2016, Rahmstorf 2007, Vermeer and Rahmstorf 2009). As such, these SEMs do not calculate sea level by resolving the underlying physical processes."

RC2.05: *Emulators and semi-empirical models are not necessarily alternatives, as the ms seems to imply (p.2). Overall, the ms does not do justice to the very large body of literature on the design, use, and potential usefulness of emulators in the field of climate change research. This comes back to haunt the ms in the discussion (e.g., page 16). Please add to the introduction a more careful review on this issue and revise the statements on this issue in the discussion. How is "robust" (p.2) defined?*

AR2.05: In order to define where the presented MAGICC sea level sits methodologically, we have referenced two different methods to efficiently estimate future sea level rise. This distinction is not meant to suggest that semi-empirical models and sea level emulators are alternatives. Both methods have their individual strengths and weaknesses and are often closely related with regards to underlying parameterizations. We have revised the manuscript to include more information on expert elicitations as well as sea level modeling methods that use paleoclimatic information to provide future projections. However, we think that providing a comprehensive discussion on "emulators in the field of climate change research" would unnecessarily lengthen the paper and distract readers interested in the sea level model description. We hope that the referee understands our reluctance to extend the introduction beyond the revised content. On p.3 l.13, we used "robust" to indicate that the calibrations for all parameterisations converge to reach their global optima (see ***AR2.10*** and ***AR2.11***). We acknowledge that this term is misleading and refined the corresponding statement. The following changes have been made to the text: p.3 l.5: "Sea level rise projections have also been provided based on expert elicitations (Horton et al. 2014). Furthermore, sea level expert judgments have been combined with statistical models synthesizing sea level projections for individual components (Kopp et al. 2014). Other studies have used an extended suite of methods, analysing paleoclimatic archives, modeling parts of the SLR response with a reduced complexity model, and deriving future projections for land ice contributions based semi-empirical considerations (Clark et al. 2016). The growing efforts in the sea level modeling community to provide fully transparent and freely available model code are reflected by the recent introduction of a transparent, simple model framework to estimate regional sea levels (Wong et al. 2017). Previous MAGICC versions provided sea level rise estimates based on parameterizations for selected components (Wigley 1995, Wigley and Raper 2005, Wigley and Raper 1987, Wigley and Raper 1992). Here, we adopt the approach of deriving a total sea level response by emulating existing process-based projections for individual sea level components (Perrette et al. 2013, Schleussner et al. 2016). Future sea level dynamics are synthesized by calibrating parameterizations to the selected complex model projections for all major sea level contributions. Progress in the understanding of individual sea level processes and the availability of revised future sea level contributions require sea level emulators to be updated regularly. With this study, we are able to complement the existing sea level projection emulators with a platform based on a comprehensive set of individual sea level components that allows for projections consistent with IPCC AR5 estimates.", p.3 l.13: "It mimics process-based sea level responses for the seven main sea level components with thoroughly calibrated parameterizations that extend global sea level projections to 2300.", p.16 l.25: "Sea level emulators complement the comprehensive but computationally expensive, process-based sea level models due to their flexible and efficient design. They can be quickly adapted to, e.g., incorporate previously unknown

uncertainties from newly quantified ice sheet processes (Clark et al. 2016, DeConto and Pollard 2016). Being directly coupled to MAGICC, our sea level model can also account for additional climate system response uncertainties and provide consistent projections for a wide range of climate change scenarios beyond the standard IPCC pathways. The latter aspects describe key strengths of the MAGICC sea level model and make it a useful tool to assess SLR for scenarios that are not covered by larger, more comprehensive models. The emulated MAGICC sea level projections reflect, independently, the reference responses for each individual sea level component, assuming that the implemented parameterizations fully capture the process-based simulations. Underlying model uncertainties differ substantially for the individual sea level components (Church et al. 2013b)."

RC2.06: *"In this study, we provide a first series of updates for MAGICC version 7 which will be consistent with the ensemble output of CMIP5" (p. 3). Is this a statement of fact or about a possible future?*

AR2.06: This is a statement of fact. Currently, the MAGICC carbon cycle is being updated. We expect the fully CMIP5-consistent MAGICC version 7 to be published by the end of this year.

RC2.07: *"The tuned model captures key features of the individual ocean heat uptake and vertical redistribution behavior of every CMIP5 model" (p. 4). Which ones?*

AR2.07: We use ocean-layer specific potential ocean temperature change as proxy for ocean heat uptake behaviour. As can be seen from Figures 2 and 3, the calibrated MAGICC ocean provides potential ocean temperature warming profiles and thermal expansion projections that are in line with the CMIP5 reference data. We have revised the statement on p.4 l.18: "The tuned model captures ocean-layer specific *thetao* change and related vertical redistribution characteristics of individual CMIP5 models, both indicators for overall ocean heat uptake behaviour."

RC2.08: *Please add a table of all model parameters, definitions, units, and values. Please review the formatting of all equations (e.g., equation 3) and symbol uses in the text (e.g., p6 l13).*

AR2.08: We have now included an overview Table A1 in the Appendix, listing key calibration variables and the calibration parameters for every sea level component. The calibration values have all been provided before in Tables 1 to 5. Thanks for notifying us about the equation formatting issues. All equations have been checked, equation 2, 3, and 6 have been updated (see also ***AR2.09***). We have included an additional sentence on p.11 l.32 to refer to the new Table: "For an overview of all relevant variables and calibration parameters please see Table A.1."

RC2.09: *Why select only 9 parameters for the calibration? How are the chosen? What would happen if you use all parameters? (p. 11)*

AR2.09: For the MAGICC ocean model calibration, we have selected all MAGICC parameters that directly determine the ocean-layer specific potential ocean temperature and corresponding thermal expansion responses. These 9 parameters drive the band-routine of the hemispheric upwelling-diffusion ocean model and are now also listed in the additional Appendix Table A.1 for clarity (see ***AR2.08***). The MAGICC sea level model calibration has been carried out per sea level contribution, only optimising the free parameters of the respective component, while prescribing the annual mean surface temperatures. As such, it was easier for us to ensure consistency with the reference data, separate the effects of individual parameter variations, and analyse the calibration quality. While carrying out additional checks of the calibration routines after the submission of the manuscript, we unfortunately discovered a bug in the MAGICC routine to prescribe annual mean surface air temperature as well as a problem with the Greenland SID functional form. Also, one specific CMIP5 model input had to be removed due to

quality issues with the reference data (BCC-CSM1.1M). All issues have been resolved. The revised prescribed temperature routine required the re-calibration of all sea level model components, with all figures now showing the corrected sea level model results. The updated optimal parameter sets are provided in the corresponding Tables. For the Greenland SID parameterisation, the calibrated constant was removed, because it prohibited reproducing lower bound projections (see revised Equation 6). In addition, the routine was adapted to allow for hindcasts without depleting the maximum outlet glacier volume, which was determined based on the year 2000. The code repository has been updated to account for these changes. We have revised the following sections to clarify the ocean model parameter selection and to account for the necessary code revisions: p.11 l.11 "Here, we select all MAGICC parameters that directly influence the ocean-layer specific potential ocean temperature and corresponding thermal expansion responses. These 9 parameters drive the band-routine of the hemispheric upwelling-diffusion ocean model", p.7 l.25 "Applying the scaling suggested by Church et al. (2013a), our total Greenland SID maximum ice discharge volumes amount to around 180 mm and 268 mm SLE for the minimum and maximum cases presented in Nick et al. (2013)", p.15 l.11 "The overall historically-constrained, probabilistic MAGICC global mean *tas* response for the 21st century is stronger than in the CMIP5 reference data for RCP4.5, RCP6.0 and RCP8.5 scenarios. This slightly steeper 21st century global mean *tas* slope is also reflected in the corresponding probabilistic MAGICC 2100 SLR estimates, given the strong air temperature dependence of the sea level model (see panels (a) to (d) of Figure 4)".

RC2.10: *Why do you choose the 5000 random parameters (I assume as a starting point)? (p. 11). Is this because there are concerns about / evidence for multiple maxima?*

AR2.10: Yes, there were concerns about local optima or too flat gradients for the optimisation routine to converge properly. Initial calibration testing with 100 initial random runs pointed to local convergence of the MAGICC ocean parameter optimisation routine. Extensive testing with 500, 1000, 5000, 7500, and 10000 initial random runs was conducted to establish the necessary number of pre-optimisation random parameter sets to appropriately map the parameter space. While all tests with 1000 parameters showed global convergence, we opted for 5000 random runs to ensure a sufficiently large set of samples for deriving the initial parameter set of the optimisation routine. The text on p.11 l.22 has been revised: "5000 random parameter sets are drawn prior to each model optimization procedure. The number of initial random runs has been determined through iterative testing to ensure convergence to a global optimum. The resulting best fit is subsequently used for the initialization of the automated Nelder-Mead simplex optimization routine (Lagarias et al. 1998, Nelder and Mead 1965) with a termination tolerance of 10^{-8} and a maximum iteration number of 10,000."

RC2.11: *You should (i) cite and discuss the ground-breaking paper: Hargreaves, J. C., and J. D. Annan (2002), Assimilation of paleo-data in a simple Earth system model, Climate Dynamics, 19(5-6), 371-381 and (ii) provide evidence for the assessment that the chosen method has a decent chance to be close to the global maximum. How are the weights for the RSS chosen (p.11, I also assume Table 1)? Is this choice consistent with the properties of the residuals?*

AR2.11: Thank you for pointing us to this relevant paper which is now cited in the revised draft. The Nelder-Mead Simplex optimisation routine as described in Lagarias et al. (1998) has been successfully applied for previous MAGICC calibration procedures (Meinshausen et al. 2011a). We are using 5000 iterations of randomly drawn calibration parameter sets to ensure that the subsequent optimisation routine shows global convergence in providing the optimal parameter fits. It is only for the ocean calibration that weights different from 1 have been applied. The different units of the ocean target variables (K for potential ocean temperatures per layer, mm for thermal expansion) call for a sensible choice of variable specific weights to not introduce an optimisation error bias for the RSS. To ensure that the calibration routine prioritises the ocean calibration while still globally converging for the thermal expansion scaling coefficient, we have iteratively derived the thermal expansion weight (0.001)

and the ocean layer temperature anomaly weight (10). The following sections of the calibration section have been revised: p.11 l.11: "Previous studies have shown that highly parameterised simple models do successfully show global convergence when calibrating a large number of free parameters (Hargreaves and Annan 2002, Meinshausen et al. 2011a)", p.11 l.26: "The *zostoga* optimization component is given four orders of magnitude less relative weight than the *thetao* component in order to prioritize the accurate layer-by-layer emulation of the respective CMIP5 model thetao time series."

RC2.12: *The claim that the presented results are "superior" (p. 16) is unclear and not backed up by evidence. Please define specific metrics (maybe hindcast cross validation error, etc.) and provide the evidence for this.*

AR2.12: We admit that "superior" should not be used in this context. However, we still think that the MAGICC sea level model has advantages over other simple sea level models that either provide a global sea level response only, e.g. semi-empirical approaches like Rahmstorf (2007), use less up-to-date reference data (Perrette et al. 2013, Schleussner et al. 2016), or do not reproduce historical data as well (Mengel et al. 2016). We have revised the corresponding statement on p.16 l.3 to now read: "The close reproduction of selected reference data (Figure 3, Figure A.3), the consistent translation of climate forcing into a SLR response within the MAGICC model, and the comprehensive representation of relevant processes (e.g. the thermal expansion contribution produced by the CMIP5-consistent MAGICC ocean model and the inclusion of the land water storage sea level component) make the MAGICC sea level model a powerful addition to the existing sea level emulators."

RC2.13: *Please review the format and missing information in the citations.*

AR2.13: Done. We have updated references which were either incomplete or not in the right format.

RC2.14: *Please show the residuals for the calibration (Figure 2). Is there a discrepancy in the lower layers? If so, how is this handled in the calibration?*

AR2.14: The calibration residuals for Figure 2 are now provided as potential ocean temperature anomalies for every MAGICC ocean layer in the Appendix, Figure A1. In addition we have decided to highlight specific model outliers in Figure 2 if they are not covered by the 90% CMIP5 reference and resulting 90% MAGICC model ranges. These figures now more clearly show what has already been stated on p.12 l.20, i.e. the tendency of the MAGICC bottom layers to warm more than the CMIP5 reference data. Calibration results for 2 of the 36 CMIP5 models show a major bottom layer warming bias. The GISS-E2-R reference data shows strong mid-layer warming combined with actual bottom layer cooling, the HadGEM2-CC data shows cooling in the upper 500 m over the historical period. In both cases, the MAGICC hemispheric upwelling-diffusion ocean model cannot fully capture these characteristics and, for the HadGEM2-CC model, overcompensates the surface cooling with strong bottom layer warming. The calibration routine itself gives all ocean layers the same weight and terminates the optimisation when the reduction in the RSS stays with the 10^{-8} termination tolerance. Both model calibration results represent the optimal parameter fits for the given reference data. We have revised the text to more clearly state these aspects. p.12 l.17 now reads: "The Figure also provides information on individual model outliers for reference data and calibration results. Corresponding potential ocean temperature residuals are shown in Figure A.1", p.12 l.18: "The updated MAGICC ocean deviates from the CMIP5 data in a few cases. Generally, there appears to be less warming in the mid-ocean between around 1500 m and 2500 m than in the CMIP5 reference data. Also, there is a tendency for the MAGICC bottom layers to warm more than the CMIP5 reference data. However, it is only for 2 of the 36 CMIP5 models used that calibration results show a major bottom layer warming bias. The GISS-E2-R reference data show strong mid-layer warming combined with actual bottom layer cooling, while the HadGEM2-CC data show cooling in the upper 500 m over the historical period (Figure A.2). In both

cases, the MAGICC hemispheric upwelling-diffusion ocean model cannot fully capture these characteristics. For the HadGEM2-CC emulation, MAGICC overcompensates the surface cooling with strong bottom layer warming." Please see also ***AR2.09***, ***AR2.10***, and ***AR2.11*** for the calibration related part of the referee comment.

RC2.15: *The fonts and line sizes in Figure 3 are too small to read. Please provide readable font sizes and line / symbol separations (as SOM if need be). Why do you choose only the 90% range for Antarctic solid ice discharge? What explains the change in range in several of the panels (e.g., a and c)? Please show the hindcasts and the residuals in for the results shown in Figure 4.*

AR2.15: Thanks for pointing this out. We have increased font size, line size, and contrast where possible to improve the readability of the Figure. Hopefully, the editor will agree to provide it as a full page graphic. We have purposefully designed the Figure in the current format to provide all calibration results in one place to allow for immediate visual checks of the calibration quality and we would like to keep this format. The ranges in each panel have been adapted to fit the projection magnitude and reference data time frame for each sea level component. This has now been stated in the caption. We only show the 90% range of the Antarctic SID component because we were not able to receive more detailed comparison data from Levermann et al. (2014). The hindcast for total SLR is now provided in Figure A.3 with three selected comparison data sets from Mengel et al. (2016), Hay et al. (2015), and Church and White (2011). The author teams of the observational datasets have been included in the acknowledgements. Hindcast for the individual SLR components have been included in Figures A.4 to A.7. For the Greenland SMB, SID and the Antarctic SMB components, the parameterisations are run freely for the historical period as the process-based model projections used as reference data do not cover this period. The historical sea level response, in particular for the GIS SID component, could be further improved in the future by also including reanalyses or observational calibration data as part of a sea level model update. This, however, is beyond the scope of the present work. We updated the text and now refer to the newly provided hindcast on p.15 l.5: "In Figure A.3, we provide MAGICC SLR hindcast results and three comparison datasets for the period 1900 to 2000. The MAGICC sea level model shows good agreement with the observational datasets based on Church and White (2011) and Hay et al. (2015). The global 1900-2300 SLR responses are provided for all RCPs and each sea level component in the Appendix Figures A.4 to A.7." Additional text has been added to the discussion section on p.16 l.3: "Our sea level model transparently emulates and combines long-term sea level projections from process-based models. It also reproduces well observed past total sea level change (see Figure A.3). Therefore, we are confident that this model contributes to advancing efficient long-term sea level projections."

References

Church, J. A., P. U. Clark, A. Cazenave, J. M. Gregory, S. Jevrejeva, A. Levermann, M. A. Merrifield, G. A. Milne, R. S. Nerem, P. D. Nunn, A. J. Payne, W. T. Pfeffer, D. Stammer & A. S. Unnikrishnan. 2013a. Sea Level Change. In *Climate Change 2013: The Physical Science Basis. Contribution of Working Group I to the Fifth Assessment Report of the Intergovernmental Panel on Climate Change,* ed. T. F. Stocker, D. Qin, G.-K. Plattner, M. Tignor, S.K. Allen, J. Boschung, A. Nauels, Y. Xia, V. Bex and P.M. Midgley. Cambridge University Press, Cambridge, United Kingdom and New York, NY, USA.

Church, J. A., D. Monselesan, J. M. Gregory & B. Marzeion (2013b) Evaluating the ability of process based models to project sea-level change. *Environmental Research Letters,* 8**,** 014051.

Church, J. A. & N. J. White (2011) Sea-Level Rise from the Late 19th to the Early 21st Century. *Surveys in Geophysics,* 32**,** 585-602.

Clark, P. U., J. D. Shakun, S. A. Marcott, A. C. Mix, M. Eby, S. Kulp, A. Levermann, G. A. Milne, P. L. Pfister, B. D. Santer, D. P. Schrag, S. Solomon, T. F. Stocker, B. H. Strauss, A. J. Weaver, R. Winkelmann, D. Archer, E. Bard, A. Goldner, K. Lambeck, R. T. Pierrehumbert & G.-K. Plattner (2016) Consequences of twenty-first-century policy for multi-millennial climate and sea-level change. *Nature Climate Change,* 6**,** 360–369.

DeConto, R. M. & D. Pollard (2016) Contribution of Antarctica to past and future sea-level rise. *Nature,* 531**,** 591-597.

Flato, G., J. Marotzke, B. Abiodun, P. Braconnot, S. C. Chou, W. Collins, P. Cox, F. Driouech, S. Emori, V. Eyring, C. Forest, P. Gleckler, E. Guilyardi, C. Jakobs, V. Kattsov, C. Reason & M. Rummukainen. 2013. Evaluation of Climate Models. In *Climate Change 2013: The Physical Science Basis. Contribution of Working Group I to the Fifth Assessment Report of the Intergovernmental Panel on Climate Change,* ed. T. F. Stocker, D. Qin, G.-K. Plattner, M. Tignor, S.K. Allen, J. Boschung, A. Nauels, Y. Xia, V. Bex and P.M. Midgley. Cambridge University Press, Cambridge, United Kingdom and New York, NY, USA.

Friedlingstein, P., M. Meinshausen, V. K. Arora, C. D. Jones, A. Anav, S. K. Liddicoat & R. Knutti (2014) Uncertainties in CMIP5 Climate Projections due to Carbon Cycle Feedbacks. *Journal of Climate,* 27**,** 511-526.

Gornitz, V., S. Lebedeff & J. Hansen (1982) Global Sea Level Trend in the Past Century. *Science,* 215**,** 1611.

Hargreaves, J. & J. Annan (2002) Assimilation of paleo-data in a simple Earth system model. *Climate Dynamics,* 19**,** 371-381.

Hay, C. C., E. Morrow, R. E. Kopp & J. X. Mitrovica (2015) Probabilistic reanalysis of twentieth-century sea-level rise. *Nature,* 517**,** 481-484.

Horton, B. P., S. Rahmstorf, S. E. Engelhart & A. C. Kemp (2014) Expert assessment of sea-level rise by AD 2100 and AD 2300. *Quaternary Science Reviews,* 84**,** 1-6.

Jevrejeva, S., J. C. Moore & A. Grinsted (2010) How will sea level respond to changes in natural and anthropogenic forcings by 2100? *Geophysical Research Letters,* 37**,** L07703.

Kopp, R. E., R. M. Horton, C. M. Little, J. X. Mitrovica, M. Oppenheimer, D. J. Rasmussen, B. H. Strauss & C. Tebaldi (2014) Probabilistic 21st and 22nd century sea-level projections at a global network of tide-gauge sites. *Earth's Future,* 2**,** 383-406.

Kopp, R. E., A. C. Kemp, K. Bittermann, B. P. Horton, J. P. Donnelly, W. R. Gehrels, C. C. Hay, J. X. Mitrovica, E. D. Morrow & S. Rahmstorf (2016) Temperature-driven global sea-level variability in the Common Era. *Proceedings of the National Academy of Sciences,* 113**,** E1434-E1441.

Lagarias, J., J. Reeds, M. Wright & P. Wright (1998) Convergence Properties of the Nelder--Mead Simplex Method in Low Dimensions. *SIAM Journal on Optimization,* 9**,** 112-147.

Levermann, A., R. Winkelmann, S. Nowicki, J. L. Fastook, K. Frieler, R. Greve, H. H. Hellmer, M. A. Martin, M. Meinshausen, M. Mengel, A. J. Payne, D. Pollard, T. Sato, R. Timmermann, W. L. Wang & R. A. Bindschadler (2014) Projecting Antarctic ice discharge using response functions from SeaRISE ice-sheet models. *Earth Syst. Dynam.,* 5**,** 271-293.

Meinshausen, M., N. Meinshausen, W. Hare, S. C. B. Raper, K. Frieler, R. Knutti, D. J. Frame & M. R. Allen (2009) Greenhouse-gas emission targets for limiting global warming to 2 degrees C. *Nature,* 458**,** 1158-1196.

Meinshausen, M., S. C. B. Raper & T. M. L. Wigley (2011a) Emulating coupled atmosphere-ocean and carbon cycle models with a simpler model, MAGICC6-Part 1: Model description and calibration. *Atmospheric Chemistry and Physics,* 11**,** 1417-1456.

Meinshausen, M., S. J. Smith, K. Calvin, J. S. Daniel, M. L. T. Kainuma, J. F. Lamarque, K. Matsumoto, S. A. Montzka, S. C. B. Raper, K. Riahi, A. Thomson, G. J. M. Velders & D. P. P. van Vuuren (2011b) The RCP greenhouse gas concentrations and their extensions from 1765 to 2300. *Climatic Change,* 109**,** 213-241.

Meinshausen, M., T. M. L. Wigley & S. C. B. Raper (2011c) Emulating atmosphere-ocean and carbon cycle models with a simpler model, MAGICC6-Part 2: Applications. *Atmospheric Chemistry and Physics,* 11**,** 1457-1471.

Mengel, M., A. Levermann, K. Frieler, A. Robinson, B. Marzeion & R. Winkelmann (2016) Future sea level rise constrained by observations and long-term commitment. *Proceedings of the National Academy of Sciences,* 113**,** 2597-2602.

Nelder, J. A. & R. Mead (1965) A Simplex Method for Function Minimization. *The Computer Journal,* 7**,** 308-313.

Nick, F. M., A. Vieli, M. L. Andersen, I. Joughin, A. Payne, T. L. Edwards, F. Pattyn & R. S. W. van de Wal (2013) Future sea-level rise from Greenland/'s main outlet glaciers in a warming climate. *Nature,* 497**,** 235-238.

Perrette, M., F. Landerer, R. Riva, K. Frieler & M. Meinshausen (2013) A scaling approach to project regional sea level rise and its uncertainties. *Earth System Dynamics,* 4**,** 11-29.

Rahmstorf, S. (2007) A semi-empirical approach to projecting future sea-level rise. *Science,* 315**,** 368-370.

Rogelj, J., M. Meinshausen & R. Knutti (2012) Global warming under old and new scenarios using IPCC climate sensitivity range estimates. *Nature Clim. Change,* 2**,** 248-253.

Rogelj, J., M. Meinshausen, J. Sedláček & R. Knutti (2014) Implications of potentially lower climate sensitivity on climate projections and policy. *Environmental Research Letters,* 9**,** 031003.

Schleussner, C. F., T. K. Lissner, E. M. Fischer, J. Wohland, M. Perrette, A. Golly, J. Rogelj, K. Childers, J. Schewe, K. Frieler, M. Mengel, W. Hare & M. Schaeffer (2016) Differential climate impacts for policy-relevant limits to global warming: the case of 1.5 °C and 2 °C. *Earth Syst. Dynam.,* 7**,** 327-351.

Vermeer, M. & S. Rahmstorf (2009) Global sea level linked to global temperature. *Proceedings of the National Academy of Sciences of the United States of America,* 106**,** 21527-21532.

Wigley, T. M. L. (1995) Global-mean temperature and sea level consequences of greenhouse gas concentration stabilization. *Geophysical Research Letters,* 22**,** 45-48.

Wigley, T. M. L. & S. C. B. Raper (1987) Thermal expansion of sea water associated with global warming. *Nature,* 330**,** 127-131.

--- (1992) Implications for climate and sea level of revised IPCC emissions scenarios. *Nature,* 357**,** 293-300.

--- (2005) Extended scenarios for glacier melt due to anthropogenic forcing. *Geophysical Research Letters,* 32.

Wong, T. E., A. Bakker, K. Ruckert, P. Applegate, A. Slangen & K. Keller (2017) BRICK v0.1, a simple, accessible, and transparent model framework for climate and regional sea-level projections. *Geosci. Model Dev. Discuss.,* 2017**,** 1-36.

Synthesizing long-term sea level rise projections - the MAGICC sea level model v2.0

Alexander Nauels[1], Malte Meinshausen[1,2], Matthias Mengel[2,3], Katja Lorbacher[1], and Tom M. L. Wigley[4,5]

[1]Australian-German Climate and Energy College, The University of Melbourne, Parkville 3010, Victoria, Australia
[2]Potsdam Institute for Climate Impact Research, Telegrafenberg A26, 14412 Potsdam, Germany
[3]Physics Institute, Potsdam University, 14476 Potsdam, Germany
[4]The Environment Institute and School of Biological Sciences, The University of Adelaide, SA 5005, Australia
[5]Climate and Global Dynamics Division, National Center for Atmospheric Research, Boulder, CO 80307-3000, USA

Correspondence to: Alexander Nauels (alexander.nauels@climate-energy-college.org)

Abstract. Sea level rise is one of the major impacts of global warming; it will threaten coastal populations, infrastructure, and ecosystems around the globe in coming centuries. Well-constrained sea level projections are needed to estimate future losses from Sea Level Rise (SLR) and benefits of climate protection and adaptation. Process-based models that are designed to resolve the underlying physics of individual sea level drivers form the basis for state-of-the-art sea level projections. However, associated computational costs allow for only a small number of simulations based on selected scenarios that often vary for different sea level components. This approach does not sufficiently support sea level impact science and climate policy advice, which require a sea level projection methodology that is flexible with regard to the climate scenario yet comprehensive and bound to the physical constraints provided by process-based models. To fill this gap, we present a sea level model that emulates global mean long-term process-based model projections for all major sea level components. Thermal expansion estimates are calculated with the hemispheric upwelling-diffusion ocean component of the simple carbon cycle-climate model MAGICC, which has been updated and calibrated against CMIP5 ocean temperature profiles and thermal expansion data. Global glacier contributions are estimated based on a parameterization constrained by transient and equilibrium process-based projections. Sea level contribution estimates for Greenland and Antarctic ice sheets are derived from surface mass balance and solid ice discharge parameterizations reproducing current output from ice-sheet models. The land water storage component replicates recent hydrological modeling results. For 2100, we project 0.35 m to 0.59 m (66% range) total SLR based on the RCP2.6 scenario, 0.45 m to 0.67 m for RCP4.5, 0.46 m to 0.71 m for RCP6.0, and 0.65 m to 0.97 m for RCP8.5. These projections lie within the range of the latest IPCC SLR estimates. SLR projections for 2300 yield median responses of 1.01 m for RCP2.6, 1.75 m for RCP4.5, 2.37 m for RCP6.0, and 4.73 m for RCP8.5. The MAGICC sea level model provides a flexible and efficient platform for the analysis of major scenario, model, and climate uncertainties underlying long-term SLR projections. It can be used as a tool to directly investigate the SLR implications of different mitigation pathways and may also serve as input for regional SLR assessments via component-wise sea level pattern scaling.

1 Introduction

Global sea level has increased by around 0.2 m since the beginning of the 20th century and will continue to rise during the 21st century and far beyond (Church and White, 2011; Church et al., 2013a). This will have wide-ranging impacts for coastal regions around the globe and therefore requires careful monitoring. The total sea level signal is the sum of several individual sea level components, the main ones being thermal expansion, global glacier melt, Greenland and Antarctic ice sheet mass loss and land water storage changes (Church et al., 2013a). Over the coming centuries, the magnitude of total SLR will strongly depend on the amount of anthropogenic Greenhouse Gases (GHG) emitted to the atmosphere during the 21st century and the corresponding physical responses of the major SLR drivers (Horton et al., 2014). Future GHG emissions are therefore a main uncertainty source when trying to project SLR trajectories. SLR uncertainties are further increased by structural differences of the underlying process-based models for the individual SLR contributions and limited process understanding, like the behavior of polar ice shelves in a warming world (Nicholls and Cazenave, 2010). To assess major parts of these scenario and model uncertainties, we extend the widely used simple carbon cycle-climate model MAGICC (Meinshausen et al., 2011a, 2009; Wigley et al., 2009; Wigley and Raper, 2001) to comprehensively model global sea level rise. This MAGICC sea level model has been designed to emulate the behavior of process-based sea level projections presented in the IPCC's Fifth Assessment Report (Church et al., 2013a), with thorough calibrations for each major sea level component. It is intended to serve as an efficient and flexible tool for the assessment of multi-centennial global sea level rise. In the following section, we motivate and explain the key concepts underlying the MAGICC sea level model. Section 2 covers the detailed model description and Section 3 provides key results. In Section 4, we discuss the capabilities of the presented sea level emulator and shine a first light on potential applications.

1.1 Motivation

Future sea level is modeled with varying degrees of complexity. Process-based modeling represents the physically most comprehensive but also computationally most expensive approach to project SLR. It is based on Atmosphere-Ocean General Circulation Models (AOGCMs) and specialized glacier, ice-sheet and ground water models that dynamically simulate sea level changes resulting from natural and anthropogenic forcings. The main sea level output from AOGCMs is the thermosteric ocean response, mostly diagnosed with post-simulation adjustments to compensate Boussinesq approximation effects (Griffies and Greatbatch, 2012). Process-based glacier and ice-sheet models are generally run separately or 'offline' and receive important boundary conditions either from observational data, AOGCMs or regional climate model input (Rae et al., 2012; Pattyn et al., 2012). Due to the complexity of the physical processes required to capture the dynamical response of each individual component, this SLR modeling approach is not feasible for efficient multi-centennial and multi-scenario research designs. It is mainly used to improve our physical understanding of the individual SLR components. The need for more efficient tools to project long-term SLR has led to the development of alternative approaches.

In the 1980s, first Semi-Empirical Models (SEMs), which estimate global sea level changes based on the evolution of global mean temperature, were introduced together with early attempts to model thermal expansion based on simplified ocean

processes (Gornitz et al., 1982). Generally, SEMs establish statistical relationships between observed/reconstructed global mean temperature or radiative forcing changes and observed/reconstructed global mean sea level changes. Assuming that such relationships stay the same for the future, they are used to estimate future SLR from projected global temperature/forcing changes (Rahmstorf, 2007; Vermeer and Rahmstorf, 2009; Jevrejeva et al., 2010; Kopp et al., 2016). As such, these SEMs do not calculate sea level by resolving the underlying physical processes. This approach generated considerable scientific debate and was not included in latest IPCC estimates (Orlic and Pasaric, 2013; Storch et al., 2008; Church et al., 2013a). The computational efficiency of this method, however, made it attractive to applied research questions, like investigating the global mean SLR response for different climate targets (Schaeffer et al., 2012). Recently, this method has been developed further and was applied to individual sea level components (Mengel et al., 2016). Sea level rise projections are also provided based on expert elicitations (Horton et al., 2014). Furthermore, sea level expert judgments have been combined with statistical models synthesizing sea level projections for individual components (Kopp et al., 2014). Other studies have used an extended suite of methods, analysing paleoclimatic archives, modeling parts of the SLR response with a reduced complexity model, and deriving future projections for land ice contributions based semi-empirical considerations (Clark et al., 2016). The growing efforts in the sea level modeling community to provide fully transparent and freely available model code are reflected by the recent introduction of a transparent, simple model framework to estimate regional sea levels (Wong et al., 2017). Previous MAGICC versions also provided sea level rise estimates based on simplified parameterizations for selected components (Wigley and Raper, 1987, 1992; Wigley, 1995; Wigley and Raper, 2005).

Here, we adopt an approach of deriving a total sea level response by emulating existing process-based projections for individual sea level components (Perrette et al., 2013; Schleussner et al., 2016). Future sea level dynamics are synthesized by calibrating simplified parameterizations to the selected complex model projections for all major sea level contributions. Progress in the understanding of individual sea level processes and the availability of revised future sea level contributions require sea level emulators to be updated regularly. With this study, we are able to complement the existing sea level projection emulators with a platform based on a comprehensive set of individual sea level components that allows for projections consistent with IPCC AR5 estimates. The MAGICC sea level model represents the first efficient sea level emulator that dynamically calculates thermal expansion with a hemispheric upwelling-diffusion model based on full hemispheric ocean temperature profiles calibrated with data from Phase 5 of the Coupled Model Intercomparison Project (CMIP5) (Taylor et al., 2012). It mimics process-based sea level responses for the seven main sea level components with thoroughly calibrated parameterizations that extend global sea level projections to 2300. Integration of the sea level model into MAGICC ensures a consistent treatment of future sea level rise and its uncertainties along the full chain from emissions to atmospheric composition, to temperature to sea level. With the option to run large ensembles in a probabilistic setup, the MAGICC sea level model allows to explore the scenario and model uncertainty space and directly investigate SLR responses associated with mitigation pathways that are not covered by the standard RCP scenarios (Moss et al., 2010). In addition, the MAGICC global SLR projections could be used for calculating regional SLR information by using them as input for pattern scaling approaches (Perrette et al., 2013).

2 Model description

The MAGICC sea level emulator (Figure 1) has been developed as an extension to the widely used MAGICC model version 6 (Meinshausen et al., 2011a, c). The MAGICC ocean model has been revised and calibrated with available CMIP5 ocean temperature and thermal expansion data. The updated MAGICC ocean provides the basis for our thermal expansion parameterization based on Lorbacher et al. (2015). Parameterizations for global glacier, Greenland Surface Mass Balance (SMB), Antarctic SMB, and Greenland Solid Ice Discharge (SID) have been calibrated against selected process-based projections for the corresponding SLR components. The linear response function approach for the Antarctic SID component presented in Levermann et al. (2014) was adapted to satisfy MAGICC model specifications. In addition, we have implemented the option to include land water SLR contribution estimates based on Wada et al. (2012) and Wada et al. (2016), with an extension until 2300.

2.1 MAGICC ocean model update and thermal expansion

MAGICC is based on a hemispheric upwelling-diffusion entrainment ocean model with depth-dependent areas for each of its 50 ocean layers (Meinshausen et al., 2011a). In this study, we provide a first series of updates for MAGICC version 7 which will be consistent with the ensemble output of CMIP5 (Taylor et al., 2012). The upwelling velocity is variable in MAGICC and the model conserves the upwelling mass flux through layer specific entrainment which is proportional to the area decrease from the top to the bottom of each layer. To avoid overestimation of ocean heat uptake for higher warming scenarios, the ocean routine includes a warming-dependent vertical diffusivity term which leads to reduced heat uptake efficiency for higher warming (Meinshausen et al., 2011a). In MAGICC6, the air temperature increases were assumed proportional to the mixed-layer ocean temperatures. A proportionality constant α (default value: 1.25) is used in earlier versions of MAGICC to account for diminishing sea ice extent in the Arctic, exposing a larger area of the (relatively warm) surface ocean waters as warming progresses with time. Here, we replace this constant factor by a term that takes into account the fact that this amplifying effect will itself diminish as the Arctic sea ice retreat is bound by the limit of a sea-ice free ocean in summer. The chosen functional form initially assumes a simple linear amplification (as in MAGICC6), and then progresses asymptotically towards a constant offset between the surface air temperature and top ocean layer warming. This new exponential adjustment term relates hemispheric air temperature change ΔT_{xA} to hemispheric mixed-layer ocean temperature change $\Delta T_{xO,1}$ as follows:

$$\Delta T_{xA} = \Delta T_{xO,1} + \eta(1 - e^{-\gamma \Delta T_{xO,1}}) \quad (1)$$

For large $\gamma \Delta T_{xO,1}$, the new sea-ice adjustment term moves towards a constant offset η between surface air temperature warming ΔT_{xA} and mixed-layer ocean warming $\Delta T_{xO,1}$. However, the surface air temperature warming initially approximates $\Delta T_{xA} = \Delta T_{xO,1}(1+\eta\gamma)$ for small $\gamma \Delta T_{x0,1}$, with $(1+\eta\gamma)$ representing the old MAGICC6 proportionality coefficient α. The sea-ice adjustment parameters η and γ are optimized together with other selected parameters for every CMIP5 model included in the MAGICC ocean model calibration (see Section 2.6). The parameter sets are optimized to represent the depth-dependent potential ocean temperature (*thetao*) responses from 36 CMIP5 models (see Table 1). The tuned model captures ocean-layer

specific *thetao* change and related vertical redistribution characteristics of individual CMIP5 models, both indicators for overall ocean heat uptake behaviour. Net ocean heat uptake can be robustly translated into thermal expansion (Kuhlbrodt and Gregory, 2012). Therefore, we can define the thermosteric response as the vertical sum of the layer-specific *thetao* anomalies multiplied by a corresponding thermal expansion coefficient α which is weighted by the specific ocean layer area. The thermal expansion coefficient α captures all relevant properties of seawater (potential seawater temperature, salinity, and pressure) that determine the corresponding sea level response (Griffies et al., 2014). For MAGICC, a simplified thermal expansion coefficient representation was developed which is solely based on *thetao* and pressure (Raper et al., 2001; Wigley et al., 2009). Recently, Lorbacher et al. (2015) have updated this parameterization to match CMIP5 thermal expansion behavior. We build our parameterization on Lorbacher et al. (2015) and calculate the thermal expansion coefficients for every MAGICC depth with the following polynomial of θ and p:

$$\alpha = (c_0 + c_1\theta_0(12.9635 - 1.0833p) - c_2\theta_1(0.1713 - 0.019263p) + c_3\theta_2(10.41 - 1.338p) + c_4p - c_5p^2)10^{-6} \quad (2)$$

The hemispheric layer specific *thetao* values θ_z are processed for every time step with $\theta_0 = \theta_z$, $\theta_1 = \theta_0^2$, and $\theta_2 = \frac{\theta_0^3}{6000}$, assuming a mean maximum ocean depth of 6000 m. The ocean depth profile, z, is translated into the pressure profile $p = 0.0098(0.1005z + 10.5exp(\frac{-1.0z}{3500} - 1.0)$, with 3500 m as the mean ocean depth. For each of the 36 MAGICC CMIP5 ocean parameter sets, the corresponding calibration parameters c_{0-5} are taken from Table S2 in Lorbacher et al. (2015). It is the combination of the CMIP5 MAGICC ocean update with the matching thermal expansion parameters that allows us to estimate 36 unique thermal expansion responses based on the selected ensemble of CMIP5 models. Our method does not cover all the spatial heterogeneity effects of thermal expansion that are seen in the three-dimensional CMIP5 fields. Therefore, we apply a model-specific scaling coefficient ϕ to the thermosteric estimates for each ocean layer to further improve the fit between the aggregated thermal expansion from the calibrated MAGICC ocean model and the CMIP5 thermosteric SLR (*zostoga*) estimates (see Section 2.6 for more details).

2.2 Global glaciers

Mountain glaciers superseded thermal expansion as the biggest single contribution to SLR by the middle of the 20th century (Gregory et al., 2013a). The global mass balance of glaciers likely turned negative in the 19th century, e.g. Leclercq et al. (2011). 20th century glacier mass loss contributed around 0.1 m of global sea level (Marzeion et al., 2012), with an increasing fraction of the glacier mass loss related to anthropogenic climatic warming, reaching around 70% in recent years (Marzeion et al., 2014). Analyses of the remaining glacier mass susceptible to melt vary from around 0.35 m Sea Level Equivalent (SLE) (Grinsted, 2013) to almost 0.5 m SLE (Marzeion et al., 2012), with both studies including peripheral glaciers of the ice sheets. The latter study is based on a glacier surface mass balance model forced with regional monthly precipitation and temperature data. Changes in glacier volume are derived with the help of volume-area scaling methods. In the follow-up study (Marzeion et al., 2014), 2300 estimates of transient glacier mass dynamics forced by 15 CMIP5 temperature and precipitation fields were complemented by equilibrium global glacier projections in response to long-term warming levels from 1 °C to 10 °C. These two experimental setups projecting transient and equilibrium glacier SLR contributions form the basis of the glacier component

that has been implemented in the MAGICC sea level model. We include Randolph Glacier Inventory 4.0 (RGI 4.0) updates on regional glacier mass loss (Pfeffer et al., 2014). The selected parameterization is based on the assumption that global glacier melt is proportional to the remaining volume susceptible to melt (at the current global temperature) times the melt forcing. This melt forcing is expressed by the temperature difference between current temperature and the temperature that would be expected if the currently remaining glacier volume was in equilibrium. Thus, we apply the following functional form to relate the global glacier SLR response GL_t to the remaining global glacier volume as well as the temperature forcing:

$$GL_t = GL_{t-1} + \kappa(V_{eq} - V_{cum})(T_t - T_{eq})^{\nu} \tag{3}$$

with calibration parameters κ and ν and V_{eq} being the equilibrium glacier volume change that would result from warming level T_t. This value is interpolated from the Marzeion et al. (2014) glacier equilibrium response data. V_{cum} is the cumulative glacier volume change since the year 1850. T_{eq} is the inverse function of the equilibrium glacier response V_{eq} to T_t and gives the temperature that would lead to the glacier volume change V_{cum} in terms of a theoretical equilibrium response.

2.3 Greenland ice sheet

The Greenland contribution to SLR increased rapidly during the last decades of the 20th century (Vaughan et al., 2013). Regional atmospheric and ocean warming has triggered wide spread surface melt (Fettweis et al., 2011) and solid ice discharge (Joughin et al., 2012). An increasingly negative SMB and a growing SLR contribution from SID, which captures accelerating ice stream flow and more frequent calving events due to warmer ocean temperatures, have been identified to be responsible for about half of the observed mass loss each (van den Broeke et al., 2009; Khan et al., 2015). The Greenland ice sheet is expected to become one of the largest SLR contributions in the future (Huybrechts et al., 2011), with potentially irreversible ice sheet loss for scenarios of persistent and strong warming (Robinson et al., 2012; Levermann et al., 2013). In the following, we present SMB and SID parameterizations that have been implemented and calibrated in the MAGICC sea level model.

2.3.1 Surface mass balance

The mass balance at the surface of the Greenland ice sheet is predominantly determined by the accumulation of snowfall in winter and runoff through melting in summer. Continuing global warming will influence the SMB through both increased snowfall and increased melting (Gregory and Huybrechts, 2006). As melting is expected to increase more strongly than snowfall, SMB losses will likely dominate future Greenland contributions to SLR (Church et al., 2013a; Goelzer et al., 2013). Regional surface air temperatures are the primary driver of these projected SMB changes if we assume future precipitation changes over Greenland to be scalable with rising temperatures (Fettweis et al., 2013; Frieler et al., 2012). Regional atmospheric temperatures are closely linked to the global mean surface air temperature *tas*. We utilize this link for our sea level component by relating two *tas* dependent terms to capture the long-term SMB sea level response. In the parameterization, the SMB response to *tas* can vary from either being approximated as scaling linearly, or non-linearly with exponent φ, or as a combination of both. The calibration procedure chooses the optimal balance of the linear and non-linear terms. Furthermore, the surface melt contribution is damped by diminishing ice availability for high warming scenarios and eventually becomes zero when all available ice is

melted. Hence, the cumulative Greenland SMB SLR contribution GIS_t^{SMB} at time step t can be written as:

$$GIS_t^{SMB} = GIS_{t-1}^{SMB} + \upsilon(\chi T_t + (1-\chi)T_t^{\varphi}) \left(1 - \frac{GIS_{t-1}^{SMB}}{GIS_{max}^{SMB}}\right)^{0.5} \quad (4)$$

The maximum Greenland ice volume available for surface melt GIS_{max}^{SMB} is about 7.36 m (Bamber et al., 2013). The overall temperature sensitivity is denoted by υ and the choice of φ sets the degree of non-linearity, while χ determines the relative magnitude of the linear and nonlinear terms. We calibrate the three parameters υ, χ, and φ with reference data from Fettweis et al. (2013). Their process-based Greenland SMB projections until 2100 are based on the regional climate model Modele Atmospherique Regional (MAR) which is coupled to the Soil Ice Snow Vegetation Atmosphere Transfer (SISVAT) scheme. The MAR model is forced by CMIP5 data for temperature, wind, humidity, and surface pressure. Comparing the MAGICC Greenland SMB response to millenial projections of Greenland ice sheet sea level contributions (Huybrechts et al., 2011; Goelzer et al., 2012) indicates that the functional form of our SMB parameterization will hold for multi-centennial projections at least until 2300.

2.3.2 Solid ice discharge

Future ocean warming is expected to reduce the frontal stress of the Greenland outlet glaciers while increased melt water from atmospheric warming can reduce the friction at the bottom of these glaciers. Both processes lead to the speed up and thinning of these glaciers, with increased discharge of solid ice into the oceans (Nick et al., 2009). Even though the SMB contribution is projected to dominate the Greenland contribution to SLR, the SID component has the potential to contribute significantly to SLR (Jacobs et al., 1992; Rignot et al., 2010; Joughin et al., 2012). Recent attempts to quantify the future ice-dynamic SLR contribution for Greenland vary widely, mainly due to different methodologies (Nick et al., 2013; Vizcaino et al., 2015; Fürst et al., 2015). We select one of the key approaches presented in the latest IPCC assessment for our reference data (Church et al., 2013a): Nick et al. (2013) use flowline modeling to project mass loss from Greenland's four main outlet glaciers, Helheim, Jakobshavn Isbrae, Kangerdluqssuaq and Petermann, until 2200. Their model is forced with ocean and atmosphere data from SRES A1B and RCP8.5 scenario runs conducted with the CMIP3 model ECHAM5-OM. As the four main outlet glaciers drain about 20% of the entire Greenland ice sheet area, the sum of the individual glacier contributions has been multiplied by a factor of 5 to estimate the SID sea level contribution of the whole ice sheet (Church et al., 2013a; Price et al., 2011). We use the same approach to emulate the response of Nick et al. (2013), with the cumulative Greenland SID SLR contribution GIS_t^{SID} at time step t being:

$$GIS_t^{SID} = s(GIS_{max}^{outlet} - GIS_{Vdis(t)}^{outlet}) \quad (5)$$

with GIS_t^{SID} defined as the difference of the initial maximum ice volume susceptible to discharge and the remaining ice volume available for discharge at time step t. Maximum ice volume, GIS_{max}^{outlet}, and remaining ice volume at time step t, $GIS_{Vdis(t)}^{outlet}$, are determined for the four main Greenland outlet glaciers. By applying the scaling factor $s = 5$, the sea level contribution is then scaled up to the entire Greenland ice sheet. For $t = 0$, $GIS_{Vdis(t=0)}^{outlet} = GIS_{max}^{outlet}$. The remaining ice

volume susceptible to discharge at time step t, $GIS^{outlet}_{Vdis(t)}$, has the following function form:

$$GIS^{outlet}_{Vdis(t)} = GIS^{outlet}_{Vdis(t-1)} - max(0, \varrho GIS^{outlet}_{Vdis(t-1)} e^{\epsilon T_{(t-1)}}) \quad (6)$$

with the annual discharge being the product of the discharge sensitivity ϱ, the SID volume $GIS^{outlet}_{Vdis(t-1)}$ available at time step $t-1$, and an exponential *tas* term which is dependent on a temperature sensitivity ϵ. We have calibrated ϱ, ϵ, and the maximum SID outlet glacier volume GIS^{outlet}_{max} based on the projected minimum and maximum contributions for dynamic retreat and thinning for scenarios SRES A1B and RCP8.5, shown in Figure 3e of Nick et al. (2013). An upper limit of the potential Greenland SID discharge contribution has not been clearly defined yet (Goelzer et al., 2013; Price et al., 2011). We include the maximum SID outlet glacier volume susceptible to discharge GIS^{outlet}_{max} in our calibration. Applying the scaling suggested by Church et al. (2013a), our total Greenland SID maximum ice discharge volumes amount to around 180 mm and 268 mm SLE for the minimum and maximum cases presented in Nick et al. (2013). For comparison, Winkelmann and Levermann (2012) obtained 420 mm for the ice-dynamic Greenland sea level contribution, indicating, however, that the actual amount might be significantly smaller. For high warming scenarios, our SID projections deplete GIS^{outlet}_{max} before the year 2300 which causes the annual Greenland SID sea level contribution to drop to zero.

2.4 Antarctic ice sheet

Air temperatures over the Antarctic ice sheet are generally much colder than over the Greenland ice sheet. They will be too low to cause wide-spread surface melting, even under strong global warming (Church et al., 2013a). Only peripheral, low-lying glaciers, especially around the Antarctic Peninsula are susceptible to retreat through increased ablation (Krinner et al., 2006). A warmer atmosphere over Antarctica will however hold more moisture, leading to higher snowfall. This effect is expected to lead to a positive SMB through snow accumulation and, thus, a slightly negative SLR contribution (Bengtsson et al., 2011; Gregory and Huybrechts, 2006). The main driver of Antarctic ice loss and a resulting positive sea level contribution is the increased melting of ice shelves through warmer ocean waters (Joughin et al., 2012; Bindschadler et al., 2013). SID will be the dominant SLR contribution of Antarctica, with increasing ocean temperatures causing basal melt in marine-based ice sheet sectors, potentially even triggering marine ice-sheet instabilities and irreversible ice loss (Huybrechts et al., 2011; Joughin et al., 2014). We implemented parameterizations capturing both, the Antarctic SMB and the SID contributions to SLR in the MAGICC SLR mode. They are presented below.

2.4.1 Surface mass balance

Positive Antarctic SMB anomalies under all warming scenarios lead to consistently negative contributions to global sea level for the 21st century. Similar to Greenland, a strong (but different) link exists between future Antarctic SMB and global mean surface air temperature *tas*. Several studies confirmed the Clausius-Clapeyron equation based exponential relationship between atmospheric warming and SMB accumulation. The values range from 3.7 % $^{\circ}C^{-1}$ (Krinner et al., 2006) up to around 7 % $^{\circ}C^{-1}$ (Bengtsson et al., 2011), with most recent estimates based on a large ensemble of climate models pointing to about 5 % $^{\circ}C^{-1}$ (Frieler et al., 2015). Ligtenberg et al. (2013) has been one of the few studies using regional climate simulations to

assess Antarctic SMB changes beyond 2100, without accounting for climate-ice sheet feedbacks however. Their assessment is based on the regional atmospheric climate model RACMO2 (Lenaerts et al., 2012) and the two global climate models ECHAM5 (Roeckner et al., 2003) and HadCM3 (Johns et al., 2003) that have been forced by two comparably moderate emission scenarios (SRES A1B and ENSEMBLES E1), leading to a 2200 Antarctic warming of 2.4-5.3 °C. Results show SMB increases of 8-25 % which translate into a global sea level drop of 73-163 mm. We select these projections as reference for our SMB parameterization. Due to the expected strong SMB link to *tas*, we have chosen a simple functional form that relates the annual Antarctic SMB sea level contribution to this primary driver:

$$AIS_t^{SMB} = AIS_{t-1}^{SMB} + \xi(\rho T_t + (1-\rho)T_t^{\sigma}) \tag{7}$$

The annual change in the Antarctic SMB contribution to SLR is derived from the sum of a linear and non-linear *tas* term, calibrated with the three parameters ξ, ρ, and σ. The transfer from global mean *tas* to regional surface air temperature changes as well as the translation of air temperatures into snowfall accumulation is captured in ξ, while ρ controls the non-linearity of the parameterization. The calibrated parameterization is then used to extend Antarctic SMB SLR estimates until 2300 presuming that the rationale behind the projections presented in Ligtenberg et al. (2013) hold for another 100 years. This is consistent with findings from up to 3000 year long Antarctic SMB simulations that are forced by idealized scenarios doubling or quadrupling atmospheric CO_2 concentration levels (Vizcaíno et al., 2010; Huybrechts et al., 2011). Results from these studies show ice mass gains due to additional snowfall for more than 500 years after the start of the experiments, e.g. see Fig. 7 in Huybrechts et al. (2011).

2.4.2 Solid ice discharge

Improved process understanding has allowed for a first assessment of the Antarctic dynamic ice-discharge contribution to SLR in the IPCC Fifth Assessment Report (Church et al., 2013a). Antarctic SID has the potential to supersede all other sea level contributions because of the vast ice masses accessible for warm ocean waters and susceptible to self-amplified retreat (DeConto and Pollard, 2016). Loss of these ice masses alone would eventually lead to several meters of global SLR (Bamber et al., 2009). Recent observations and modeling suggests that the process of self-sustained retreat has already begun and will dominate over the slower adjustments to *tas* and precipitation changes across the Antarctic continent on decadal to centennial timescales (Joughin et al., 2014; Rignot et al., 2014; Favier et al., 2014). Levermann et al. (2014) convolve the responses from five different Antarctic ice-sheet models to basal melt forcing as used in the SeaRISE project (Bindschadler et al., 2013) with a large set of MAGICC temperature projections for the full suite of RCP scenarios. In their study, the projected global mean *tas* signal is converted into subsurface ocean temperatures that are translated into basal melt forcing. The melt forcing is then convolved with individual response functions for the Amundsen Sea, Ross Sea, Weddell Sea, and East Antarctic sectors. This approach is well suited for the MAGICC sea level model implementation because it relates the ice-sheet response directly to *tas*. We implement a step-wise convolution routine in the MAGICC SLR model which allows us to process the response functions for the different sectors. The total SLR contribution from Antarctic SID, AIS^{SID}, can be written as the sum of the

contributions from the individual sectors:

$$AIS^{SID} = \sum_{n=1}^{4} \int_{0}^{t} F_n(\tau) R_n(t-\tau)\,\mathrm{d}\tau \tag{8}$$

The sector-specific basal melt forcing F_n is the product of the basal melt sensitivity ψ and the sector-specific subsurface ocean temperature anomaly dT_{OCN}. The region-specific ice sheet response function $R_n(t-\tau)$ is based on linear response theory (Winkelmann and Levermann, 2012). The basal melt forcing F is the product of the basal melt sensitivity ψ and the sector-specific subsurface ocean temperature anomaly dT_{OCN}. Starting in 1850, Levermann et al. (2014) derived the latter from the projected annual MAGICC global mean *tas* anomalies via ocean temperature scaling and a time delay between surface and ocean subsurface warming. We adopt all relevant melt forcing parameters from Levermann et al. (2014). They determined these parameters either through calibrations against 19 CMIP5 models or adopted them from the existing literature, like the basal melt sensitivities ranging from 7 $ma^{-1}K^{-1}$ to 16 $ma^{-1}K^{-1}$ (Holland et al., 2008; Payne et al., 2007; Jenkins, 1991). The response functions are derived for 500 years and cover the time frame of their source experiments described in Bindschadler et al. (2013). We provide Antarctic SID projections up to the year 2300. For the MAGICC component, it is only response functions from the three ice-sheet models that have an explicit representation of ice-shelf dynamics that are included, namely PennState-3D (Pollard and DeConto, 2012), PISM (Winkelmann et al., 2011; Martin et al., 2011), and SICOPOLIS (Sato and Greve, 2012). The response functions presented by Levermann et al. (2014) and implemented here do not account for all ice sheet processes and feedbacks. Thus, the Antarctic SID estimates provided by the MAGICC sea level model may underestimate the actual Antarctic SID sea level response.

2.5 Land water storage

The assessment of the observed and projected anthropogenic land water contribution to SLR is subject to ongoing discussions (Konikow, 2011; Pokhrel et al., 2012; Wada et al., 2012; Church et al., 2013a; Wada et al., 2016). Associated uncertainties are high, mainly due to sparse data coverage and incomplete process understanding. Two major processes drive changes in land water storage: the depletion of groundwater resources which positively contributes to SLR; and water impoundment which damps the SLR signal. Analyses show that the latter contribution has been shrinking since the late 20th century (Gregory et al., 2013b) which leaves groundwater depletion as the main human-driven Land Water Storage (LWS) SLR contribution throughout the 21st century and beyond. We include the option to provide LWS sea level estimates based on the approach introduced by Wada et al. (2012). They forced the hydrological model PCR-GLOBWB (van Beek et al., 2011) with climate projections from AOGCMs to derive estimates for future groundwater depletion until 2100. Original estimates had to be revised because only roughly 80% of annually depleted groundwater ends up in the oceans (Wada et al., 2016). We adapt our time series accordingly, reducing the Wada et al. (2012) sea level contribution estimates from groundwater depletion by 20%. We use the 30-year average annual depletion rate for the period 2071-2100 to extend the projections beyond the 21st century. We assume that projected rates of human water use and groundwater abstraction, which show more constant rates towards the end of the 21st century (Wada, 2015), will persist beyond 2100. The fraction of non-renewable groundwater to total groundwater

abstraction is projected to increase to around 50% by 2100 (Wada, 2015). This indicates that, ultimately, the total amount of groundwater available for abstraction is limited. To account for such an upper bound of the LWS sea level contribution, we use a term that relates the cumulative LWS contribution to a theoretical maximum LWS volume that can be depleted. No distinction is made between different climate scenarios for the post-2100 LWS extension due to the limited process understanding and the associated large uncertainties (Church et al., 2013a). Hence, we implement the revised Wada et al. (2012) estimates until 2100 and apply the following post-2100 LWS parameterization:

$$LWS_t = LWS_{t-1} + LWS_{const}\left(1 - \frac{LWS_{t-1} - LWS_{2100}}{LWS_{max} - LWS_{2100}}\right)^{0.5} \quad (9)$$

The maximum LWS volume LWS_{max} has not been quantified yet de Graaf et al. (2014). However, Gleeson et al. (2015) quantified the amount of modern groundwater which is defined as less than 50 year old groundwater located in the top 2 km of the continental crust. This type of groundwater dominates the interaction with general hydrological cycle and the climate system. It is also the most accessible for land use (Gleeson et al., 2015). We here define LWS_{max} as the total amount of available modern groundwater which has been estimated to be around 350,000 km^3, roughly translating to 1000 mm SLE.

2.6 Model calibration

For the MAGICC ocean model calibration, we use two CMIP5 variables for our reference data set: ocean potential temperatures (*thetao*) and thermal expansion (*zostoga*). Ocean depths specific *thetao* time series are extracted for a total of 36 CMIP5 models which have been running pre-industrial control (*pictrl*), historical, some or all of the RCP experiments as well as the idealized 1% CO2 per year increase (*1pctCO2*) experiments. Each individual model output is converted into hemispheric annual mean *thetao* depth profile time series that are then vertically interpolated to match the MAGICC ocean layer depths. We combine historical and RCP runs to create layer-specific time series from 1850 to 2100 or 2300 depending on the experiment lengths of the individual CMIP5 model runs. Ocean temperature data available from the CMIP archives are subject to drift because the time scales for the ocean to adjust to external forcing are much longer than the length of the control experiments (Taylor et al., 2012; Gupta et al., 2013). Individual model drifts have been identified based on the respective *pictrl* runs. The full linear trend from the *pictrl* experiments has been removed from the historical plus RCP and *1pctCO2* scenario time series.

The initial *thetao* profiles are prescribed for every CMIP5 model calibration as well as the respective depth-dependent ocean area fractions. We incorporate *zostoga* estimates for each of the 36 CMIP5 ensemble members by detrending the times series with the full linear trend of the *pictrl* runs. To ensure a full CMIP5-consistent calibration setup, we constrain MAGICC for every CMIP5 model optimization by prescribing the corresponding model-specific annual global mean surface air temperature *tas*. Previous studies have shown that highly parameterised simple models do successfully show global convergence when calibrating a large number of free parameters (Hargreaves and Annan, 2002; Meinshausen et al., 2011a). Here, we select all MAGICC parameters which directly determine the ocean-layer specific potential ocean temperature and corresponding thermal expansion responses. These 9 parameters drive the band-routine of the hemispheric upwelling-diffusion ocean model. The vertical thermal diffusivity, K_z, its sensitivity to global-mean surface temperatures at the mixed layer boundary, $\frac{dK_{z_{top}}}{dT}$, the sea-ice adjustment parameters η and γ described above, the initial upwelling rate w_0, the ratio of changes in the temperature

of the entraining waters to those of the polar sinking waters β, the ratio of variable to fixed upwelling for every time step $\frac{\Delta w_t}{w_t}$, and the corresponding threshold temperatures that lead to constant upwelling rates, namely T_{w_t}, and the global thermal expansion scaling coefficient ϕ. More details on the individual parameters can be found in Meinshausen et al. (2011a) except for the sea-ice adjustment variables described in Section 2.1. For every CMIP5 model, this suite of calibration parameters is optimized based on the scenario specific CMIP5 *thetao* data for the representative layers 1 (30m layer mean depth), 2 (110m), 3(210m), 8 (710m), 15 (1410m), 30 (2910m), and 40 (3910m), and the corresponding *zostoga* time series. The eight calibration layers have been selected to allow the MAGICC ocean model to emulate the key features of the CMIP5 ocean temperature profiles, with the majority of calibration layers set in the upper ocean to ensure sufficient coverage of the stronger temperature gradients. The number of reference layers is not increased further to preserve computational efficiency. 5000 random parameter sets are drawn prior to each model optimization procedure. The number of initial random runs has been determined through iterative testing to ensure convergence to a global optimum. The resulting best fit is subsequently used for the initialization of the automated Nelder-Mead simplex optimization routine (Lagarias et al., 1998; Nelder and Mead, 1965) with a termination tolerance of 10^{-8} and a maximum iteration number of 10,000. We use weighted Residual Sum of Squares (RSS) for Goodness-Of-Fit (GOF) diagnostics during the optimization process (Meinshausen et al., 2011a). The ocean calibration also takes into account the available CMIP5 *zostoga* time series. The *zostoga* optimization component is given four orders of magnitude less relative weight than the *thetao* component in order to prioritize the accurate layer-by-layer emulation of the respective CMIP5 model *thetao* time series. The GOF values are then divided by the number of calibrated model years, accounting for the varying amount of scenario data available for each model. This allows us to compare the GOFs of the calibrations for all 36 CMIP5 models.

The calibration procedures for the other SLR components also optimize the specific parameters listed in Tables 2 to 5 based on the Nelder-Mead Simplex method with a termination tolerance of 10^{-8} for a change in RSS during the last iteration. For an overview of all relevant variables and calibration parameters please see Table A.1. All the remaining SLR components use reference SLE contributions in millimeters for the respective optimizations. For the glacier contribution, the MAGICC sea level response is fitted to the transient Marzeion et al. (2014) projections. The free parameters κ and ν are calibrated for each of the 14 CMIP5 reference models and their respective combined historical and RCP simulations, starting in 1850. Corresponding CMIP5 global mean *tas* projections are prescribed in the MAGICC model to ensure consistency with CMIP5. We use a subset of the model specific 1965-2100 projections made available by Fettweis et al. (2013) to calibrate the parameterization for the Greenland SMB contribution. 24 CMIP5 models are selected based on the availability of CMIP5 *tas* projections for the scenarios RCP4.5 and RCP8.5. We then prescribe these global mean *tas* time series for the calibration procedure of the three parameters υ, χ, and φ. Calibration data for the Greenland SID component is only available for one GCM, ECHAM5. For the optimization of the parameters ϱ, ϵ, and GIS_{max}^{outlet}, global mean *tas* runs for SRES A1B and RCP8.5 are used with 2200 extensions, repeating the last decade of the 21st century ten times (Nick et al., 2013). The calibration of the Antarctic SMB component is based on process-based SLR responses forced by two GCMs (Ligtenberg et al., 2013). In this reference study, ECHAM5 and HadCM3 model output was applied for scenarios SRES A1B and ENSEMBLES E1. We replicate these GCM responses and use the provided Antarctic SMB sea level contributions starting in 1980 to determine the optimal parameters

ξ, ρ, σ. The Antarctic SID as well as the LWS components are not subject to calibration procedures as they apply the same method of the reference study in the case of Antarctic SID or simply include and extend the reference data for LWS.

3 Results

The MAGICC ocean model update yields optimal parameter sets for every CMIP5 model used in the calibration procedure outlined above. Those sets are listed in Table 1. In Figure 2, we show both the 90% model range and the median for the reference CMIP5 global potential ocean temperature anomalies as well as the median MAGICC global ocean warming profile averaged over 2081 to 2100 relative to the reference period 1986 to 2005. The Figure also provides information on individual model outliers for reference data and calibration results. Corresponding potential ocean temperature residuals are shown in Figure A.1. MAGICC is able to capture the key CMIP5 features for all RCP scenarios. The median model response either matches or is close to the median of the CMIP5 responses. The updated MAGICC ocean deviates from the CMIP5 data in a few cases. Generally, there appears to be less warming in the mid-ocean between around 1500 m and 2500 m than in the CMIP5 reference data. Also, there is a tendency for the MAGICC bottom layers to warm more than the CMIP5 reference data. However, it is only for 2 of the 36 CMIP5 models used that calibration results show a major bottom layer warming bias. The GISS-E2-R reference data show strong mid-layer warming combined with actual bottom layer cooling, while the HadGEM2-CC data show cooling in the upper 500 m over the historical period (see Figure A.2). In both cases, the MAGICC hemispheric upwelling-diffusion ocean model cannot fully capture these characteristics. For the HadGEM2-CC emulation, MAGICC overcompensates the surface cooling with strong bottom layer warming. Apart from these anomalies, the calibrated MAGICC ocean component captures the hemispherically averaged CMIP5 ocean warming for the different RCP scenarios well (Figure 2, Figure A.1). We derive CMIP5 consistent thermal expansion estimates based on the optimal ocean parameter sets and the additional thermal expansion scaling parameter ϕ (see Table 1).

In Figure 3, we synthesize the calibration results for all sea level contributions captured by the MAGICC sea level model. Panels (a) to (d) show the model specific global thermal expansion responses and the corresponding CMIP5 *zostoga* reference data for the four RCP scenarios. The number of available reference runs differs for each scenario as does the length of the simulations. The updated MAGICC ocean component is able to mimic the CMIP5 thermal expansion time series. Relative to 1850, the calibration yields a 2100 thermosteric SLR range of 104 to 238 mm (CMIP5: 113 to 231 mm) for RCP2.6, 151 to 307 mm (161 to 290 mm) for RCP4.5 , 166 to 331 mm (174 to 309 mm) for RCP6.0, and 219 to 491 mm (261 to 445 mm) for RCP8.5. The corresponding 1850 to 2300 thermosteric SLR responses range from 192 to 335 mm for RCP2.6 (CMIP5: 180 to 288 mm), 348 to 709 mm for RCP4.5 (345 to 707 mm), 586 to 717 mm for RCP6.0 (635 to 658 mm), and 1040 to 1794 mm for RCP8.5 (1040 to 1909 mm). In contrast to some detrended *zostoga* CMIP5 model time series, the MAGICC thermal expansion projections do not show negative slopes in the 20th century which is consistent with observations (Church et al., 2013b).

The calibrated global glacier SLR response and the corresponding reference data are shown in panels (e) to (h), while the specific calibration results are listed in Table 2. The MAGICC projections show good agreement with the updated Marzeion et al. (2012) data (Fig. 3, panels (e) to (h)). Relative to 1850, the estimated glacier SLE contributions in 2100 are 145 to 259

mm (Marzeion et al.: 134 to 256 mm) for RCP2.6, 162 to 276 mm (159 to 277 mm) for RCP4.5, 163 to 276 (163 to 276 mm) for RCP6.0, and 188 to 302 mm (198 to 308 mm) for RCP8.5. For 2300, projected SLR from glaciers amounts to a SLE range of 177 to 298 mm (Marzeion et al.: 188 to 305 mm) for RCP2.6, 255 to 374 mm (254 to 366 mm) for RCP4.5, and 325 to 439 mm (338 to 444 mm) for RCP8.5.

In panels (j) and (k), we cover the Greenland SMB contribution, both the reference data from Fettweis et al. (2013) and the sea level model estimates based on the optimal paramester sets shown in Table 3. Our model shows high agreement with the reference data. For 2100, we project SLE ranges from 18 to 117 mm (Fettweis et al.: 17 to 114 mm) based on RCP4.5 and SLE ranges from 49 to 208 (48 to 206 mm) based on RCP8.5. Projections start in 1965, being the first year of the calibration data. The Greenland SID calibration results are depicted in panels (l) and (m) of Figure 3. We show MAGICC sea level model estimates based on the calibration results listed in Table 4. As presented by Nick et al. (2013), we show projections of the minimum and maximum cases for the combined contribution from the four major outlet glaciers prior to up-scaling to the entire Greenland ice sheet. Estimates are provided relative to the year 2000. For the SRES A1B scenario, the SLE projections range from 17 to 28 mm (Nick et al.: 14 to 25 mm) for the last year of the available reference data in 2190. For the same year, we project 24 to 42 mm (26 to 43 mm) based on the RCP8.5 scenario.

Calibration results for the Antarctic SMB component which negatively contributes to future SLR are listed in Table 5. Corresponding output is shown in panels (n) and (o). Starting in 1980, the reference data from Ligtenberg et al. (2013) provides projections that go beyond 2100 only for the model HadCM3. For the ENSEMBLES E1 scenario, the two model specific 2100 SLE responses range from -29 to -18 mm (Ligtenberg et al.: -27 to -20 mm). The 2200 estimate lies at -67 mm (-73 mm) based on the HadCM3 parameter set. The 2100 values for the SRES A1B scenario span from -51 to -33 mm (Ligtenberg et al.: -44 to -32 mm), while the 2200 Antarctic SMB SLE response is projected to be -158 mm (-163 mm). As we model the Antarctic SID sea level component with the linear response function approach presented by Levermann et al. (2014), it is not calibrated against any reference data. The MAGICC component utilizes the responses from the three ice-sheet models of that study which include an explicit representation of ice-shelf dynamics. As the sea level responses for this subset of ice-shelf models are not available, we show the 90% model range and the median of all five ice-sheet models from Levermann et al. (2014) in panels (p) to (s) of Figure 3. CMIP5 model specific parameter sets have been determined for the three different ice-shelf models (Levermann et al. (2014), Tables 2-5). For 1850 to 2100, the 90% ranges of the MAGICC responses based on the ice-shelf model subset correspond to 33 to 253 mm SLE (Levermann et al.: 15 to 227 mm) for RCP2.6, 39 to 319 mm (17 to 267 mm) for RCP4.5, 42 to 338 mm (17 to 277 mm) for RCP6.0, and 53 to 448 mm (20 to 365 mm) for RCP8.5. For 1850 to 2300, 90% of the MAGICC projections lie within 115 and 874 mm SLE (Levermann et al.: 69 to 635 mm) for RCP2.6, 209 and 1435 mm (119 to 1182 mm) for RCP4.5, 282 and 1860 mm (161 to 1719 mm) for RCP6.0, and 505 and 3173 mm (300 to 3535 mm) for RCP8.5, respectively. The MAGICC Antarctic SID estimates, which are based on the physically more complex ice-shelf models only, mostly lie within the 90% range of Antarctic SID sea level contributions provided by Levermann et al. (2014).

In panel (t), we show SLE responses for the scenario independent land water SLE component. From 1900 to 2100, we include the net land water SLE contribution as presented in Figure 3 of Wada et al. (2012), corrected by the 20% fraction of land water that does not reach the global ocean Wada et al. (2016). Post 2100, we assume a constant annual contribution based

on the assumptions outlined in section (2.5). 2100 estimates span a global sea level contribution of 39 to 77 mm. The extended land water projections range from 156 to 261 mm SLE for 2300.

With the individual SLR components calibrated, we can project total SLR as the combination of the individual SLE responses from each of the seven sea level components. Two different MAGICC setups are used to project global SLR until 2100 and 2300 based on the four RCP scenarios and their extensions. The ocean model update is not sufficient to make the MAGICC model fully CMIP5 consistent because other crucial climate system components like the carbon cycle have not been updated yet. To overcome this issue, we constrain the MAGICC model with available CMIP5 global mean *tas* time series. Together with the corresponding calibrated MAGICC ocean model parameter sets, we are able to create a CMIP5 environment that allows us to compare our 2100 global SLR projections to the latest IPCC estimates. Beyond 2100, the number of available CMIP5 simulations is much smaller, with only two 2300 model runs available for RCP6.0, for example. In order to also provide a sufficiently large number of model runs for 2300, we use 600 historically-constrained parameter sets that have been derived using a probabilistic Metropolis-Hastings Markov chain Monte Carlo method (Meinshausen et al., 2009). This approach has been extended to also reflect carbon-cycle uncertainties (Friedlingstein et al., 2014) and the climate sensitivity range of the latest IPCC assessment (Flato et al., 2013; Rogelj et al., 2012, 2014). For this second setup, MAGICC is not forced to match CMIP5 global mean *tas*, allowing us to provide consistent ensemble projections out to 2300. For this ensemble, we randomly draw from the CMIP5 ocean model parameter sets and the calibration results for each sea level model component. Random samples are also sourced between the minimum and maximum realizations for the Greenland SID and LWS component as well as between the empirical basal melt sensitivities for the Antarctic SID contribution (Levermann et al., 2014). For consistency, we adopt the same ensemble size for the CMIP5 constrained MAGICC setup and randomly select the specific CMIP5 global mean *tas* time series in addition to the other randomized parameter sets from the individual sea level components.

In Table 6, we show median SLR estimates for the 2081-2100 average relative to 1986-2005 and 66% ranges for every individual component, with corresponding IPCC reference estimates and likely ranges. The individual MAGICC sea level contributions are in good agreement with the IPCC estimates. Figure 4 shows the full suite of MAGICC SLR projections for the RCP scenarios. The smaller panels (a) to (d) give 90% and 66% ranges as well as median responses for all RCP scenarios until 2100 based on the CMIP5 consistent setup. Additional bars are provided for the IPCC reference data and the probabilistic MAGICC setup which is not constrained to CMIP5. For the CMIP5 consistent MAGICC setup, 2100 median SLR is projected to be 0.45 m (66% range: 0.35 m to 0.59 m) for RCP2.6, 0.55 m (0.45 m to 0.67 m) for RCP4.5, 0.56 m for (0.46 m to 0.71 m) for RCP6.0, and 0.79 m (0.65 m to 0.97 m) for RCP8.5 (see also Table 7). All SLR projections are provided relative to the reference period 1986 to 2005. MAGICC SLR estimates for 2100 are generally higher than the IPCC projections. CMIP5 consistent projections of average 2081 to 2100 SLR lie well withing the IPCC range, with median estimates on average 0.02 m higher than the corresponding IPCC values (Church et al., 2013a). In panel (e), we provide 2300 SLR projections for the RCP extensions based on the probabilistic MAGICC setup which is not constrained to CMIP5. For RCP2.6, the median SLR reponse is 1.01 m (66% range: 0.80 to 1.35 m). We project a median of 1.75 m (1.29 to 2.30 m) for RCP4.5, 2.37 m (1.72 to 3.20 m) for RCP6.0, and up to 4.73 m (3.41 to 6.83 m) for RCP8.5 (see also Table 7). In Figure A.3, we provide MAGICC SLR hindcast results and three comparison datasets for the period 1900 to 2000. The MAGICC sea level model shows good

agreement with the observational datasets based on Church et al. (2011) and Hay et al. (2015). The global 1900-2300 SLR responses are provided for all RCPs and each sea level component in the Appendix Figures A.4 to A.7.

Figure 5 shows the global mean *tas* responses based on the historically-constrained, probabilistic MAGICC setup, which is used for the 2300 SLR projections. Each panel also includes the available CMIP5 global mean *tas* time series. 2300 MAGICC median global mean *tas* fall well within the available CMIP5 range for RCP4.5, RCP6.0 and RCP8.5. The MAGICC median global mean *tas* response is at the lower end of 2300 CMIP5 temperatures for RCP2.6. For this scenario, the projected cooling over 22nd and 23rd centuries is consistent with previous MAGICC studies, e.g. Meinshausen et al. (2011b). The overall historically-constrained, probabilistic MAGICC global mean *tas* response for the 21st century is stronger than in the CMIP5 reference data for RCP4.5, RCP6.0 and RCP8.5 scenarios. This slightly steeper 21st century global mean *tas* slope is also reflected in the corresponding probabilistic MAGICC 2100 SLR estimates, given the strong air temperature dependence of the sea level model (see panels (a) to (d) of Figure 4).

4 Discussion

The MAGICC sea level model presented here synthesizes long-term sea level projections for seven sea level components and provides up-to-date and efficient representations of the individual SLR contributions, validated against process-based model results (see Figure 3 and Section 2). Thermal expansion is calculated with an updated version of the MAGICC hemispheric upwelling-diffusion ocean model and an ocean-layer specific thermal expansion parameterization by Lorbacher et al. (2015). We are therefore able to directly account for ocean heat uptake effects, which is an advantage over other contribution-based approaches that simply derive thermal expansion from global mean air temperature changes (Mengel et al., 2016). The MAGICC ocean thermal expansion component is calibrated to be fully consistent with CMIP5. The glacier component parameterization accounts for both transient projections of glacier mass loss (Marzeion et al., 2012) and equilibrium glacier responses based on Marzeion et al. (2014). The SMB and SID parameterizations for both ice sheets reflect available process-based reference data (Fettweis et al., 2013; Nick et al., 2013; Ligtenberg et al., 2013; Levermann et al., 2014). In addition, new process understanding has been included in the land water component (Wada et al., 2016). The full MAGICC model, including the sea level module, can be run in less than one second for 100 model years on a single core. This makes it an efficient platform to provide large ensembles of global sea level projections.

Projecting SLR beyond 2100 and providing physically-consistent global estimates out to 2300 has been one of the key motivations for the development of the MAGICC sea level model. For five of the seven sea level components, the reference data used for calibrating the individual contributions extend beyond 2100. For thermal expansion, global glacier, and Antarctic SID contributions, the reference calibration period spans from 1850 to 2300. The remaining components are based on physically plausible assumptions, which allow us to also provide 2300 estimates, assuming that the calibrated parameterizations for each sea level component remain valid. Our sea level model transparently emulates and combines long-term sea level projections from process-based models. It also reproduces well observed past total sea level change (see Figure A.3). Therefore, we are confident that this model contributes to advancing efficient long-term sea level projections. The close reproduction of selected

reference data (Figure 3, Figure A.3), the consistent translation of climate forcing into a SLR response within the MAGICC model, and the comprehensive representation of relevant processes (e.g. the thermal expansion contribution produced by the CMIP5-consistent MAGICC ocean model and the inclusion of the land water storage sea level component) make the MAGICC sea level model a powerful addition to the existing sea level emulators.

Both CMIP5 ocean and air temperatures serve as input for the presented sea level model. Other published sea level emulators only utilize air temperature projections, also provided by MAGICC, either based purely on available CMIP3 calibration results (Meinshausen et al., 2011a; Perrette et al., 2013) or an updated historically-constrained probabilistic MAGICC setup that reflects the latest IPCC climate sensitivity estimates (Schleussner et al., 2016; Mengel et al., 2016). We here provide the first major step to making MAGICC fully CMIP5 consistent, with the ocean model now emulating 36 CMIP5 hemispheric potential ocean temperature and thermal expansion responses. However, other crucial elements of the MAGICC model, like the atmosphere and the carbon cycle, are not yet calibrated to CMIP5. When combining the CMIP5-calibrated ocean with the older atmosphere and carbon cycle calibrations, the resulting 21st century warming is slightly stronger than CMIP5 (see Figure 5). To ensure a robust MAGICC sea level model, the individual components were either calibrated with prescribed CMIP5 temperatures, or with CMIP3 consistent time series whenever the reference data was based on the older generation of SRES and ENSEMBLES scenarios. The quality of the sea level model calibration is therefore not affected by the warmer MAGICC air temperature response. Our primary 2100 SLR projections are based on a MAGICC ensemble that is constrained by CMIP5 global mean *tas*. These projections can therefore be directly compared to recent IPCC estimates. For our 2300 projections, we run MAGICC in the historically-constrained, probabilistic setup described above. The resulting MAGICC air temperature responses mostly reflect the available CMIP5 reference data, although they show a shorter response time scale (see Figure 5). These differences to CMIP5 translate into the corresponding SLR projections due to the strong air temperature dependence of the sea level model. Hence, the MAGICC sea level module will only be able to provide fully CMIP5 consistent SLR responses for 2300 once the remaining components of the MAGICC model have been updated.

Sea level emulators complement the comprehensive but computationally expensive, process-based sea level models due to their flexible and efficient design. They can be quickly adapted to, e.g., incorporate previously unknown uncertainties from newly quantified ice sheet processes (Clark et al., 2016; DeConto and Pollard, 2016). Being directly coupled to MAGICC, our sea level model can also account for additional climate system response uncertainties and provide consistent projections for a wide range of climate change scenarios beyond the standard IPCC pathways. The latter aspects describe key strengths of the MAGICC sea level model and make it a useful tool to assess SLR for scenarios that are not covered by larger, more comprehensive models. The emulated MAGICC sea level projections reflect, independently, the reference responses for each individual sea level component, assuming that the implemented parameterizations fully capture the process-based simulations. Underlying model uncertainties differ substantially for the individual sea level components (Church et al., 2013b). In 2300, the three largest model response uncertainties captured by the MAGICC sea level model for RCP8.5 are the Greenland SMB component with 66% range estimates of 0.74 m to 2.51 m, the thermal expansion component with a 66% range of 1.07 m to 2.65 m, and the Antarctic SID component with 0.65 m to 1.85 m. Emulators, as presented here, can only cover the uncertainty ranges that are reflected in the emulated process-based models. Even though there have been substantial advances in process

understanding over the last years, the physical representation of some sea level contributions remains incomplete. The Antarctic ice sheet response, for example, could be subject to more rapid, non-linear dynamics that are not captured by current process-based projections. Only recently, DeConto and Pollard (2016) have revised potential future Antarctic contributions to global sea level based on indicators from paleoclimatic archives. For RCP8.5, they suggest 2100 contributions of around 1m from Antarctica alone, with 2300 contributions reaching up to around 10 m. The MAGICC sea level model projections for the Antarctic SID contribution are based on Levermann et al. (2014) and only yield up to around 0.35 m in 2100 and 2.68 m in 2300 for the upper bound of the 90% range. As the more recent research suggests, these estimates may be too low, indicating that the Antarctic contribution to future SLR is subject to additional uncertainties. This illustrates the need to handle long-term SLR projections with care and to note the corresponding methodological caveats; in particular, those surrounding the representation of Antarctic ice-sheet changes.

The MAGICC sea level model assesses long-term global SLR trajectories by synthesizing available process-based projections for the individual sea level drivers and applying them to the available set of RCP scenarios and their extensions until 2300. The current version shows 2100 estimates that are well within the range of the latest IPCC assessment (see Figure 4). The structure of the emulator makes the MAGICC sea level model a computationally much more efficient tool compared to the comprehensive and complex process-based models. The calibration routines for the individual components have been flexibly designed to allow for timely updates whenever new robust modeling results become available. The presented MAGICC sea level model, together with the MAGICC ocean model update, are new elements of MAGICC model version 6 (Meinshausen et al., 2011a). The implementation of the new sea level model initiates the development of MAGICC model version 7 to comprehensively emulate CMIP5 projections. The full potential of the MAGICC sea level model will be unlocked once this MAGICC model upgrade has been completed.

Model code and data availabilty

The Fortran code of the MAGICC sea level model together with its documentation is available here: https://gitlab.com/anauels/MAGICC_SLR_model.

CMIP5 model output is freely available from the PCMDI database: http://cmip-pcmdi.llnl.gov/. Corresponding calibration input data as well as output from the conducted experiments is available on request. Component-specific additional reference datasets should be requested from the authors of the individual studies.

Author contributions. A. Nauels developed and calibrated the sea level model with support from M. Meinshausen, M. Mengel, and K. Lorbacher. A. Nauels conducted the experiments and drafted the manuscript. All authors contributed to the text and declare that they have no conflict of interest.

Acknowledgements. We acknowledge the World Climate Research Programme's Working Group on Coupled Modeling, which is responsible for CMIP, and we thank the climate modeling groups for producing and making available their model output (CMIP5 models used in the

present study are listed in Table 1 of this paper, see also http://cmip-pcmdi.llnl.gov/cmip5/docs/CMIP5_modeling_groups.pdf). For CMIP the U.S. Department of Energy's Program for Climate Model Diagnosis and Intercomparison provides coordinating support and led development of software infrastructure in partnership with the Global Organization for Earth System Science Portals. We would especially like to thank B. Marzeion, X. Fettweis, F. Nick, S. Ligtenberg, A. Levermann, and Y. Wada for providing the calibration data used in this study. The authors would also like to acknowledge C. Hay and J. Church and the CSIRO for making available their GMSL reconstruction/reanalysis datasets. M. Meinshausen receives the Australian Research Council (ARC) Future Fellowship Grant FT130100809. T. M. L. Wigley is supported by the Australian Research Council under Discovery Grant DP130103261.

References

Bamber, J. L., Riva, R. E. M., Vermeersen, B. L. A., and LeBrocq, A. M.: Reassessment of the Potential Sea-Level Rise from a Collapse of the West Antarctic Ice Sheet, Science, 324, 901–903, 2009.

Bamber, J. L., Griggs, J. A., Hurkmans, R. T. W. L., Dowdeswell, J. A., Gogineni, S. P., Howat, I., Mouginot, J., Paden, J., Palmer, S., Rignot, E., and Steinhage, D.: A new bed elevation dataset for Greenland, The Cryosphere, 7, 499–510, 2013.

Bengtsson, L., Koumoutsaris, S., and Hodges, K.: Large-Scale Surface Mass Balance of Ice Sheets from a Comprehensive Atmospheric Model, Surveys in Geophysics, 32, 459–474, 2011.

Bindschadler, R. A., Nowicki, S., Abe-Ouchi, A., Aschwanden, A., Choi, H., Fastook, J., Granzow, G., Greve, R., Gutowski, G., Herzfeld, U., Jackson, C., Johnson, J., Khroulev, C., Levermann, A., Lipscomb, W. H., Martin, M. A., Morlighem, M., Parizek, B. R., Pollard, D., Price, S. F., Ren, D., Saito, F., Sato, T., Seddik, H., Seroussi, H., Takahashi, K., Walker, R., and Wang, W. L.: Ice-sheet model sensitivities to environmental forcing and their use in projecting future sea level (the SeaRISE project), Journal of Glaciology, 59, 195–224, 2013.

Church, J. A. and White, N. J.: Sea-Level Rise from the Late 19th to the Early 21st Century, Surveys in Geophysics, 32, 585–602, 2011.

Church, J. A., Gregory, J. M., White, N. J., Platten, S. M., and Mitrovica, J. X.: Understanding and Projecting Sea Level Change, Oceanography, 24, 130–143, 2011.

Church, J. A., Clark, P., Cazenave, A., Gregory, J., Jevrejeva, S., Levermann, A., Merrifield, M., Milne, G., Nerem, R., Nunn, P., Payne, A., Pfeffer, W., Stammer, D., Unnikrishnan, A., (eds.) Stocker, T. F., Qin, D., Plattner, G.-K., Tignor, M., Allen, S. K., Boschung, J., Nauels, A., Xia, Y., Bex, V., and Midgley, P. M.: Sea Level Change. In: Climate Change 2013: The Physical Science Basis. Contribution of Working Group I to the Fifth Assessment Report of the Intergovernmental Panel on Climate Change, chap. 13, Cambridge University Press, Cambridge, United Kingdom and New York, NY, USA, 2013a.

Church, J. A., Monselesan, D., Gregory, J. M., and Marzeion, B.: Evaluating the ability of process based models to project sea-level change, Environmental Research Letters, 8, 014 051, 2013b.

Clark, P. U., Shakun, J. D., Marcott, S. A., Mix, A. C., Eby, M., Kulp, S., Levermann, A., Milne, G. A., Pfister, P. L., Santer, B. D., Schrag, D. P., Solomon, S., Stocker, T. F., Strauss, B. H., Weaver, A. J., Winkelmann, R., Archer, D., Bard, E., Goldner, A., Lambeck, K., Pierrehumbert, R. T., and Plattner, G.-K.: Consequences of twenty-first-century policy for multi-millennial climate and sea-level change, Nature Climate Change, 6, 360–369, 2016.

de Graaf, I., van Beek, L., Wada, Y., and Bierkens, M.: Dynamic attribution of global water demand to surface water and groundwater resources: Effects of abstractions and return flows on river discharges, Advances in Water Resources, 64, 21–33, 2014.

DeConto, R. M. and Pollard, D.: Contribution of Antarctica to past and future sea-level rise, Nature, 531, 591–597, 2016.

Favier, L., Durand, G., Cornford, S. L., Gudmundsson, G. H., Gagliardini, O., Gillet-Chaulet, F., Zwinger, T., Payne, A. J., and Le Brocq, A. M.: Retreat of Pine Island Glacier controlled by marine ice-sheet instability, Nature Clim. Change, 4, 117–121, 2014.

Fettweis, X., Tedesco, M., van den Broeke, M., and Ettema, J.: Melting trends over the Greenland ice sheet (1958-2009) from spaceborne microwave data and regional climate models, The Cryosphere, 5, 359–375, 2011.

Fettweis, X., Franco, B., Tedesco, M., van Angelen, J. H., Lenaerts, J. T. M., van den Broeke, M. R., and Gallée, H.: Estimating the Greenland ice sheet surface mass balance contribution to future sea level rise using the regional atmospheric climate model MAR, The Cryosphere, 7, 469–489, 2013.

Flato, G., Marotzke, J., Abiodun, B., Braconnot, P., Chou, S., Collins, W., Cox, P., Driouech, F., Emori, S., Eyring, V., Forest, C., Gleckler, P., Guilyardi, E., Jakobs, C., Kattsov, V., Reason, C., Rummukainen, M., (eds.) Stocker, T. F., Qin, D., Plattner, G.-K., Tignor, M., Allen,

S. K., Boschung, J., Nauels, A., Xia, Y., Bex, V., and Midgley, P. M.: Evaluation of Climate Models. In: Climate Change 2013: The Physical Science Basis. Contribution of Working Group I to the Fifth Assessment Report of the Intergovernmental Panel on Climate Change, chap. 9, Cambridge University Press, Cambridge, United Kingdom and New York, NY, USA, 2013.

Friedlingstein, P., Andrew, R. M., Rogelj, J., Peters, G. P., Canadell, J. G., Knutti, R., Luderer, G., Raupach, M. R., Schaeffer, M., van Vuuren, D. P., and Le Quere, C.: Persistent growth of CO2 emissions and implications for reaching climate targets, Nature Geosci, 7, 709–715, 2014.

Frieler, K., Meinshausen, M., Mengel, M., Braun, N., and Hare, W.: A Scaling Approach to Probabilistic Assessment of Regional Climate Change, Journal of Climate, 25, 3117–3144, 2012.

Frieler, K., Mengel, M., and Levermann, A.: Delaying future sea-level rise by storing water on Antarctica, Earth Syst. Dynam. Discuss., 6, 1979–1997, 2015.

Fürst, J. J., Goelzer, H., and Huybrechts, P.: Ice-dynamic projections of the Greenland ice sheet in response to atmospheric and oceanic warming, The Cryosphere, 9, 1039–1062, 2015.

Gleeson, T., Befus, K. M., Jasechko, S., Luijendijk, E., and Cardenas, M. B.: The global volume and distribution of modern groundwater, Nature Geoscience, 9, 161–167, 2015.

Goelzer, H., Huybrechts, P., Raper, S. C. B., Loutre, M.-F., Goosse, H., and Fichefet, T.: Millennial total sea-level commitments projected with the Earth system model of intermediate complexity LOVECLIM, Environmental Research Letters, 7, 045 401, 2012.

Goelzer, H., Huybrechts, P., Furst, J. J., Nick, F. M., Andersen, M. L., Edwards, T. L., Fettweis, X., Payne, A. J., and Shannon, S.: Sensitivity of Greenland ice sheet projections to model formulations, Journal of Glaciology, 59, 733–749, 2013.

Gornitz, V., Lebedeff, S., and Hansen, J.: Global Sea Level Trend in the Past Century, Science, 215, 1611–1614, 1982.

Gregory, J. and Huybrechts, P.: Ice-sheet contributions to future sea-level change, Philosophical Transactions of the Royal Society A: Mathematical, Physical and Engineering Sciences, 364, 1709–1732, 2006.

Gregory, J. M., Bi, D., Collier, M. A., Dix, M. R., Hirst, A. C., Hu, A., Huber, M., Knutti, R., Marsland, S. J., Meinshausen, M., Rashid, H. A., Rotstayn, L. D., Schurer, A., and Church, J. A.: Climate models without preindustrial volcanic forcing underestimate historical ocean thermal expansion, Geophysical Research Letters, 40, 1600–1604, 2013a.

Gregory, J. M., White, N. J., Church, J. A., Bierkens, M. F. P., Box, J. E., van den Broeke, M. R., Cogley, J. G., Fettweis, X., Hanna, E., Huybrechts, P., Konikow, L. F., Leclercq, P. W., Marzeion, B., Oerlemans, J., Tamisiea, M. E., Wada, Y., Wake, L. M., and van de Wal, R. S. W.: Twentieth-Century Global-Mean Sea Level Rise: Is the Whole Greater than the Sum of the Parts?, Journal of Climate, 26, 4476–4499, 2013b.

Griffies, S. M. and Greatbatch, R. J.: Physical processes that impact the evolution of global mean sea level in ocean climate models, Ocean Modelling, 51, 37–72, 2012.

Griffies, S. M., Yin, J., Durack, P. J., Goddard, P., Bates, S. C., Behrens, E., Bentsen, M., Bi, D., Biastoch, A., Böning, C. W., Bozec, A., Chassignet, E., Danabasoglu, G., Danilov, S., Domingues, C. M., Drange, H., Farneti, R., Fernandez, E., Greatbatch, R. J., Holland, D. M., Ilicak, M., Large, W. G., Lorbacher, K., Lu, J., Marsland, S. J., Mishra, A., George Nurser, A. J., Salas y Mélia, D., Palter, J. B., Samuels, B. L., Schröter, J., Schwarzkopf, F. U., Sidorenko, D., Treguier, A. M., Tseng, Y.-h., Tsujino, H., Uotila, P., Valcke, S., Voldoire, A., Wang, Q., Winton, M., and Zhang, X.: An assessment of global and regional sea level for years 1993–2007 in a suite of interannual CORE-II simulations, Ocean Modelling, 78, 35–89, 2014.

Grinsted, A.: An estimate of global glacier volume, The Cryosphere, 7, 141–151, 2013.

Gupta, A. S., Jourdain, N. C., Brown, J. N., and Monselesan, D.: Climate Drift in the CMIP5 Models, Journal of Climate, 26, 8597–8615, 2013.

Hargreaves, J. and Annan, J.: Assimilation of paleo-data in a simple Earth system model, Climate Dynamics, 19, 371–381, 2002.

Hay, C. C., Morrow, E., Kopp, R. E., and Mitrovica, J. X.: Probabilistic reanalysis of twentieth-century sea-level rise, Nature, 517, 481–484, 2015.

Holland, P. R., Jenkins, A., and Holland, D. M.: The response of ice shelf basal melting to variations in ocean temperature, Journal of Climate, 21, 2558–2572, 2008.

Horton, B. P., Rahmstorf, S., Engelhart, S. E., and Kemp, A. C.: Expert assessment of sea-level rise by AD 2100 and AD 2300, Quaternary Science Reviews, 84, 1–6, 2014.

Huybrechts, P., Goelzer, H., Janssens, I., Driesschaert, E., Fichefet, T., Goosse, H., and Loutre, M. F.: Response of the Greenland and Antarctic Ice Sheets to Multi-Millennial Greenhouse Warming in the Earth System Model of Intermediate Complexity LOVECLIM, Surveys in Geophysics, 32, 397–416, 2011.

Jacobs, S. S., Helmer, H. H., Doake, C. S. M., Jenkins, A., and Frolich, R. M.: Melting of Ice Shelves and the Mass Balance of Antarctica, Journal of Glaciology, 38, 375–387, 1992.

Jenkins, A.: A one-dimensional model of ice shelf-ocean interaction, Journal of Geophysical Research: Oceans, 96, 20 671–20 677, 1991.

Jevrejeva, S., Moore, J. C., and Grinsted, A.: How will sea level respond to changes in natural and anthropogenic forcings by 2100?, Geophysical Research Letters, 37, l07703, 2010.

Johns, T. C., Gregory, J. M., Ingram, W. J., Johnson, C. E., Jones, A., Lowe, J. A., Mitchell, J. F. B., Roberts, D. L., Sexton, D. M. H., Stevenson, D. S., Tett, S. F. B., and Woodage, M. J.: Anthropogenic climate change for 1860 to 2100 simulated with the HadCM3 model under updated emissions scenarios, Climate Dynamics, 20, 583–612, 2003.

Joughin, I., Alley, R. B., and Holland, D. M.: Ice-Sheet Response to Oceanic Forcing, Science, 338, 1172–1176, 2012.

Joughin, I., Smith, B. E., and Medley, B.: Marine Ice Sheet Collapse Potentially Under Way for the Thwaites Glacier Basin, West Antarctica, Science, 344, 735–738, 2014.

Khan, S. A., Aschwanden, A., Bjørk, A. A., Wahr, J., Kjeldsen, K. K., and Kjær, K. H.: Greenland ice sheet mass balance: a review, Reports on Progress in Physics, 78, 046 801, 2015.

Konikow, L. F.: Contribution of global groundwater depletion since 1900 to sea-level rise, Geophysical Research Letters, 38, l17401, 2011.

Kopp, R. E., Horton, R. M., Little, C. M., Mitrovica, J. X., Oppenheimer, M., Rasmussen, D. J., Strauss, B. H., and Tebaldi, C.: Probabilistic 21st and 22nd century sea-level projections at a global network of tide-gauge sites, Earth's Future, 2, 383–406, 2014.

Kopp, R. E., Kemp, A. C., Bittermann, K., Horton, B. P., Donnelly, J. P., Gehrels, W. R., Hay, C. C., Mitrovica, J. X., Morrow, E. D., and Rahmstorf, S.: Temperature-driven global sea-level variability in the Common Era, Proceedings of the National Academy of Sciences, 113, 1434–1441, 2016.

Krinner, G., Magand, O., Simmonds, I., Genthon, C., and Dufresne, J. L.: Simulated Antarctic precipitation and surface mass balance at the end of the twentieth and twenty-first centuries, Climate Dynamics, 28, 215–230, 2006.

Kuhlbrodt, T. and Gregory, J. M.: Ocean heat uptake and its consequences for the magnitude of sea level rise and climate change, Geophysical Research Letters, 39, l18608, 2012.

Lagarias, J., Reeds, J., Wright, M., and Wright, P.: Convergence Properties of the Nelder–Mead Simplex Method in Low Dimensions, SIAM J. Optim., 9, 112–147, 1998.

Leclercq, P. W., Oerlemans, J., and Cogley, J. G.: Estimating the Glacier Contribution to Sea-Level Rise for the Period 1800-2005, Surveys in Geophysics, 32, 519–535, 2011.

Lenaerts, J. T. M., van den Broeke, M. R., van de Berg, W. J., van Meijgaard, E., and Kuipers Munneke, P.: A new, high-resolution surface mass balance map of Antarctica (1979–2010) based on regional atmospheric climate modeling, Geophysical Research Letters, 39, 2012.

Levermann, A., Clark, P. U., Marzeion, B., Milne, G. A., Pollard, D., Radic, V., and Robinson, A.: The multimillennial sea-level commitment of global warming, Proceedings of the National Academy of Sciences, 2013.

Levermann, A., Winkelmann, R., Nowicki, S., Fastook, J. L., Frieler, K., Greve, R., Hellmer, H. H., Martin, M. A., Meinshausen, M., Mengel, M., Payne, A. J., Pollard, D., Sato, T., Timmermann, R., Wang, W. L., and Bindschadler, R. A.: Projecting Antarctic ice discharge using response functions from SeaRISE ice-sheet models, Earth Syst. Dynam., 5, 271–293, 2014.

Ligtenberg, S. R. M., van de Berg, W. J., van den Broeke, M. R., Rae, J. G. L., and van Meijgaard, E.: Future surface mass balance of the Antarctic ice sheet and its influence on sea level change, simulated by a regional atmospheric climate model, Climate Dynamics, 41, 867–884, 2013.

Lorbacher, K., Nauels, A., and Meinshausen, M.: Complementing thermosteric sea level rise estimates, Geosci. Model Dev., 8, 2723–2734, 2015.

Martin, M. A., Winkelmann, R., Haseloff, M., Albrecht, T., Bueler, E., Khroulev, C., and Levermann, A.: The Potsdam Parallel Ice Sheet Model (PISM-PIK) - Part 2: Dynamic equilibrium simulation of the Antarctic ice sheet, The Cryosphere, 5, 727–740, 2011.

Marzeion, B., Jarosch, A. H., and Hofer, M.: Past and future sea-level change from the surface mass balance of glaciers, The Cryosphere, 6, 1295–1322, 2012.

Marzeion, B., Cogley, J. G., Richter, K., and Parkes, D.: Attribution of global glacier mass loss to anthropogenic and natural causes, Science, 345, 919–921, 2014.

Meinshausen, M., Meinshausen, N., Hare, W., Raper, S. C. B., Frieler, K., Knutti, R., Frame, D. J., and Allen, M. R.: Greenhouse-gas emission targets for limiting global warming to 2 degrees C, Nature, 458, 1158–1162, 2009.

Meinshausen, M., Raper, S. C. B., and Wigley, T. M. L.: Emulating coupled atmosphere-ocean and carbon cycle models with a simpler model, MAGICC6 - Part 1: Model description and calibration, Atmospheric Chemistry and Physics, 11, 1417–1456, 2011a.

Meinshausen, M., Smith, S. J., Calvin, K., Daniel, J. S., Kainuma, M. L. T., Lamarque, J. F., Matsumoto, K., Montzka, S. A., Raper, S. C. B., Riahi, K., Thomson, A., Velders, G. J. M., and van Vuuren, D. P. P.: The RCP greenhouse gas concentrations and their extensions from 1765 to 2300, Climatic Change, 109, 213–241, 2011b.

Meinshausen, M., Wigley, T. M. L., and Raper, S. C. B.: Emulating atmosphere-ocean and carbon cycle models with a simpler model, MAGICC6-Part 2: Applications, Atmospheric Chemistry and Physics, 11, 1457–1471, 2011c.

Mengel, M., Levermann, A., Frieler, K., Robinson, A., Marzeion, B., and Winkelmann, R.: Future sea level rise constrained by observations and long-term commitment, Proceedings of the National Academy of Sciences, 113, 2597–2602, 2016.

Moss, R. H., Edmonds, J. A., Hibbard, K. A., Manning, M. R., Rose, S. K., van Vuuren, D. P., Carter, T. R., Emori, S., Kainuma, M., Kram, T., Meehl, G. A., Mitchell, J. F. B., Nakicenovic, N., Riahi, K., Smith, S. J., Stouffer, R. J., Thomson, A. M., Weyant, J. P., and Wilbanks, T. J.: The next generation of scenarios for climate change research and assessment, Nature, 463, 747–756, 2010.

Nelder, J. A. and Mead, R.: A simplex method for function minimization, Computer Journal, 7, 308–313, 1965.

Nicholls, R. J. and Cazenave, A.: Sea-Level Rise and Its Impact on Coastal Zones, Science, 328, 1517–1520, 2010.

Nick, F. M., Vieli, A., Howat, I. M., and Joughin, I.: Large-scale changes in Greenland outlet glacier dynamics triggered at the terminus, Nature Geosci, 2, 110–114, 2009.

Nick, F. M., Vieli, A., Andersen, M. L., Joughin, I., Payne, A., Edwards, T. L., Pattyn, F., and van de Wal, R. S. W.: Future sea-level rise from Greenland's main outlet glaciers in a warming climate, Nature, 497, 235–238, 2013.

Orlic, M. and Pasaric, Z.: Semi-empirical versus process-based sea-level projections for the twenty-first century, Nature Clim. Change, 3, 735–738, 2013.

Pattyn, F., Schoof, C., Perichon, L., Hindmarsh, R. C. A., Bueler, E., de Fleurian, B., Durand, G., Gagliardini, O., Gladstone, R., Goldberg, D., Gudmundsson, G. H., Huybrechts, P., Lee, V., Nick, F. M., Payne, A. J., Pollard, D., Rybak, O., Saito, F., and Vieli, A.: Results of the Marine Ice Sheet Model Intercomparison Project, MISMIP, The Cryosphere, 6, 573–588, 2012.

Payne, A. J., Holland, P. R., Shepherd, A. P., Rutt, I. C., Jenkins, A., and Joughin, I.: Numerical modeling of ocean-ice interactions under Pine Island Bay's ice shelf, Journal of Geophysical Research: Oceans, 112, 2007.

Perrette, M., Landerer, F., Riva, R., Frieler, K., and Meinshausen, M.: A scaling approach to project regional sea level rise and its uncertainties, Earth System Dynamics, 4, 11–29, 2013.

Pfeffer, W. T., Arendt, A. A., Bliss, A., Bolch, T., Cogley, J. G., Gardner, A. S., Hagen, J.-O., Hock, R., Kaser, G., Kienholz, C., Miles, E. S., Moholdt, G., Mölg, N., Paul, F., Radi, Valentina, Rastner, P., Raup, B. H., Rich, J., and Sharp, M. J.: The Randolph Glacier Inventory: a globally complete inventory of glaciers, Journal of Glaciology, 60, 537–552, 2014.

Pokhrel, Y. N., Hanasaki, N., Yeh, P. J. F., Yamada, T. J., Kanae, S., and Oki, T.: Model estimates of sea-level change due to anthropogenic impacts on terrestrial water storage, Nature Geosci, 5, 389–392, 2012.

Pollard, D. and DeConto, R. M.: Description of a hybrid ice sheet-shelf model, and application to Antarctica, Geoscientific Model Development, 5, 1273–1295, 2012.

Price, S. F., Payne, A. J., Howat, I. M., and Smith, B. E.: Committed sea-level rise for the next century from Greenland ice sheet dynamics during the past decade, Proceedings of the National Academy of Sciences, 2011.

Rae, J. G. L., Aðalgeirsdóttir, G., Edwards, T. L., Fettweis, X., Gregory, J. M., Hewitt, H. T., Lowe, J. A., Lucas-Picher, P., Mottram, R. H., Payne, A. J., Ridley, J. K., Shannon, S. R., van de Berg, W. J., van de Wal, R. S. W., and van den Broeke, M. R.: Greenland ice sheet surface mass balance: evaluating simulations and making projections with regional climate models, The Cryosphere, 6, 1275–1294, 2012.

Rahmstorf, S.: A semi-empirical approach to projecting future sea-level rise, Science, 315, 368–370, 2007.

Raper, S. C. B., Gregory, J. M., and Osborn, T. J.: Use of an upwelling-diffusion energy balance climate model to simulate and diagnose A/OGCM results, Climate Dynamics, 17, 601–613, 2001.

Rignot, E., Koppes, M., and Velicogna, I.: Rapid submarine melting of the calving faces of West Greenland glaciers, Nature Geoscience, 3, 187–191, 2010.

Rignot, E., Mouginot, J., Morlighem, M., Seroussi, H., and Scheuchl, B.: Widespread, rapid grounding line retreat of Pine Island, Thwaites, Smith, and Kohler glaciers, West Antarctica, from 1992 to 2011, Geophysical Research Letters, 41, 3502–3509, 2014.

Robinson, A., Calov, R., and Ganopolski, A.: Multistability and critical thresholds of the Greenland ice sheet, Nature Climate Change, 2, 429–432, 2012.

Roeckner, E., Baeuml, G., Bonaventura, L., Brokopf, R., Esch, M., Giorgetta, M., Hagemann, S., Kirchner, I., Kornblueh, L., Manzini, E., Rhodin, A., Schlese, U., Schulzweida, U., and Tompkins, A.: The atmospheric general circulation model ECHAM 5. PART I: Model description, Report No. 349, Tech. rep., Max-Planck-Institut fuer Meteorologie, Hamburg, 2003.

Rogelj, J., Meinshausen, M., and Knutti, R.: Global warming under old an new scenarios using IPCC climate sensitivity range estimates, Nature Climate Change, 2, 248–253, 2012.

Rogelj, J., Meinshausen, M., Sedláček, J., and Knutti, R.: Implications of potentially lower climate sensitivity on climate projections and policy, Environmental Research Letters, 9, 031 003, 2014.

Sato, T. and Greve, R.: Sensitivity experiments for the Antarctic ice sheet with varied sub-ice-shelf melting rates, Annals of Glaciology, 53, 221–228, 2012.

Schaeffer, M., Hare, W., Rahmstorf, S., and Vermeer, M.: Long-term sea-level rise implied by 1.5 degrees C and 2 degrees C warming levels, Nature Climate Change, 2, 867–870, 2012.

Schleussner, C.-F., Lissner, T. K., Fischer, E. M., Wohland, J., Perrette, M., Golly, A., Rogelj, J., Childers, K., Schewe, J., Frieler, K., Mengel, M., Hare, W., and Schaeffer, M.: Differential climate impacts for policy-relevant limits to global warming: the case of 1.5 °C and 2°C, Earth System Dynamics, 7, 327–351, 2016.

Storch, H., Zorita, E., and González-Rouco, J.: Relationship between global mean sea-level and global mean temperature in a climate simulation of the past millennium, Ocean Dynamics, 58, 227–236, 2008.

Taylor, K. E., Stouffer, R. J., and Meehl, G. A.: An Overview of CMIP5 and the Experiment Design, Bulletin of the American Meteorological Society, 93, 485–498, 2012.

van Beek, L. P. H., Wada, Y., and Bierkens, M. F. P.: Global monthly water stress: 1. Water balance and water availability, Water Resources Research, 47, w07517, 2011.

van den Broeke, M., Bamber, J., Ettema, J., Rignot, E., Schrama, E., van de Berg, W. J., van Meijgaard, E., Velicogna, I., and Wouters, B.: Partitioning Recent Greenland Mass Loss, Science, 326, 984–986, 2009.

Vaughan, D. G., Comiso, J., Allison, I., Carrasco, J., Kaser, G., Kwok, R., Mote, P., Murray, T., Paul, F., Ren, D., Rignot, E., Solomina, O., Steffen, K., Zhang, N., (eds.) Stocker, T. F., Qin, D., Plattner, G.-K., Tignor, M., Allen, S. K., Boschung, J., Nauels, A., Xia, Y., Bex, V., and Midgley, P. M.: Observations: Cryosphere. In: Climate Change 2013: The Physical Science Basis. Contribution of Working Group I to the Fifth Assessment Report of the Intergovernmental Panel on Climate Change, chap. 4, Cambridge University Press, Cambridge, United Kingdom and New York, NY, USA, 2013.

Vermeer, M. and Rahmstorf, S.: Global sea level linked to global temperature, Proceedings of the National Academy of Sciences of the United States of America, 106, 21 527–21 532, 2009.

Vizcaino, M., Mikolajewicz, U., Ziemen, F., Rodehacke, C. B., Greve, R., and van den Broeke, M. R.: Coupled simulations of Greenland Ice Sheet and climate change up to A.D. 2300, Geophysical Research Letters, 42, 3927–3935, 2015.

Vizcaíno, M., Mikolajewicz, U., Jungclaus, J., and Schurgers, G.: Climate modification by future ice sheet changes and consequences for ice sheet mass balance, Climate Dynamics, 34, 301–324, 2010.

Wada, Y.: Modeling Groundwater Depletion at Regional and Global Scales: Present State and Future Prospects, Surveys in Geophysics, pp. 1–33, 2015.

Wada, Y., van Beek, L. P. H., Sperna Weiland, F. C., Chao, B. F., Wu, Y.-H., and Bierkens, M. F. P.: Past and future contribution of global groundwater depletion to sea-level rise, Geophysical Research Letters, 39, L09 402, 2012.

Wada, Y., Lo, M.-H., Yeh, P. J. F., Reager, J. T., Famiglietti, J. S., Wu, R.-J., and Tseng, Y.-H.: Fate of water pumped from underground and contributions to sea-level rise, Nature Climate Change, 6, 777–780, 2016.

Wigley, T. M. L.: Global-mean temperature and sea level consequences of greenhouse gas concentration stabilization, Geophys. Res. Lett., 22, 45–48, 1995.

Wigley, T. M. L. and Raper, S. C. B.: Thermal expansion of sea water associated with global warming, Nature, 330, 127–131, 1987.

Wigley, T. M. L. and Raper, S. C. B.: Implications for climate and sea level of revised IPCC emissions scenarios, Nature, 357, 293–300, 1992.

Wigley, T. M. L. and Raper, S. C. B.: Interpretation of High Projections for Global-Mean Warming, Science, 293, 451–454, 2001.

Wigley, T. M. L. and Raper, S. C. B.: Extended scenarios for glacier melt due to anthropogenic forcing, Geophysical Research Letters, 32, 2005.

Wigley, T. M. L., Clarke, L. E., Edmonds, J. A., Jacoby, H. D., Paltsev, S., Pitcher, H., Reilly, J. M., Richels, R., Sarofim, M. C., and Smith, S. J.: Uncertainties in climate stabilization, Climatic Change, 97, 85–121, 2009.

Winkelmann, R. and Levermann, A.: Linear response functions to project contributions to future sea level, Climate Dynamics, 40, 2579–2588, 2012.

Winkelmann, R., Martin, M. A., Haseloff, M., Albrecht, T., Bueler, E., Khroulev, C., and Levermann, A.: The Potsdam Parallel Ice Sheet Model (PISM-PIK) - Part 1: Model description, The Cryosphere, 5, 715–726, 2011.

Wong, T. E., Bakker, A., Ruckert, K., Applegate, P., Slangen, A., and Keller, K.: BRICK v0.1, a simple, accessible, and transparent model framework for climate and regional sea-level projections, Geoscientific Model Development Discussions, pp. 1–36, 2017.

Table 1. MAGICC ocean model calibration results with optimal sets of ocean and thermal expansion calibration parameters for the available CMIP5 models. Calibration parameters are introduced in section 2.6. Goodness-Of-Fit (GOF) results are given as weighted Residual Sum of Squares (RSS) divided by the number of calibrated model years (weight potential ocean temperature [K]: 10, weight thermal expansion [mm]: 0.001). The optimal set for the mean response of the calibration data is given at the bottom of the table.

Model	K_z	$\frac{dK_{z_{top}}}{dT}$	η	γ	β	w_0	$\frac{\Delta w_t}{w_t}$	T_{w_t}	ϕ	GOF
ACCESS1.0	4.3846	-1.3441	2.4191	0.2954	0.1997	0.0678	0.9999	1.9021	1.1141	0.11
ACCESS1.3	0.1792	-0.0249	4.5743	0.0806	0.0598	9.959	0.2044	3.0533	1.1277	0.08
BCC-CSM1.1	1.3457	0.0701	2.223	0.2245	0.2348	0.0100	0.9506	16.417	1.0303	0.11
BNU-ESM	1.9336	-0.4034	3.5734	0.2422	0.6824	2.9546	0.0010	4.5004	1.2220	0.13
CanESM2	0.9065	0.2868	5.0000	0.1132	0.1259	1.171	0.7481	8.1589	1.0857	0.16
CCSM4	1.1155	0.2327	1.6218	0.3368	0.0132	1.2702	0.3359	1.5202	1.0321	0.15
CESM1-BGC	1.1713	-0.0654	3.2018	0.1302	0.1024	9.986	0.223	3.8928	1.0533	0.03
CESM1-CAM5	0.0100	0.8004	2.5411	0.2834	0.0767	1.9277	0.7618	16.873	1.0993	0.13
CMCC-CESM	0.4599	-0.0209	1.8620	0.2551	0.0100	10.000	0.4610	9.4486	1.1590	0.13
CMCC-CM	1.4137	-0.4317	1.0552	0.9129	0.2519	1.9925	0.9999	19.599	0.9382	0.10
CMCC-CMS	0.0105	-0.7989	4.9992	0.0807	0.1531	9.9999	0.2939	4.7474	0.9858	0.05
CNRM-CM5	0.1377	0.1547	3.2070	0.1776	0.4134	0.5078	0.8680	1.3343	1.0254	0.20
CNRM-CM5-2	1.3200	-0.2081	5.0000	0.1146	0.1037	0.6386	0.8098	1.7782	1.4547	0.05
CSIRO-Mk3.6.0	2.0085	-0.0361	3.7756	0.1510	0.0137	0.0117	0.1865	17.812	1.0633	0.49
EC-EARTH	2.5850	-0.6157	4.9892	0.1077	0.2489	2.4364	0.0720	19.999	1.0624	0.05
GFDL-CM3	0.0329	0.3796	5.0000	0.1638	0.0599	2.9073	0.3461	2.3735	1.1692	0.18
GFDL-ESM2G	2.6329	-1.4040	2.1535	0.2304	1.0000	2.2037	0.8837	20.000	1.3555	0.15
GFDL-ESM2M	2.9547	1.0000	4.9372	0.1387	0.1479	0.0101	0.5316	7.4830	1.1790	0.11
GISS-E2-H	1.2987	0.3002	1.5682	0.4334	0.0334	0.5996	0.9527	2.4943	1.1256	0.07
GISS-E2-HCC	0.0107	1.0000	1.4129	0.6907	0.3571	3.7715	0.9091	17.974	1.0928	0.11
GISS-E2-R	0.9151	0.9383	1.6601	0.4458	0.1069	1.0556	1.0000	1.5897	1.0861	0.17
GISS-E2-RCC	4.9680	-1.0529	1.484	0.5898	0.1609	1.3509	0.2843	1.3137	1.1696	0.12
HadGEM2-CC	0.4727	-0.0493	2.8069	0.1638	0.5988	4.6183	0.0246	1.2449	1.3297	0.07
HadGEM2-ES	0.6165	0.0620	3.4649	0.2123	0.3212	2.9456	0.2779	2.3299	1.1488	0.39
IPSL-CM5A-LR	1.0928	-0.0191	3.1337	0.1181	0.2414	1.8789	0.3740	11.705	1.0677	0.10
IPSL-CM5A-MR	1.0047	-0.0643	1.5549	0.3573	0.9473	0.7214	1.0000	15.414	1.0472	0.09
IPSL-CM5B-LR	1.6262	0.0318	5.0000	0.1234	0.0262	6.5424	0.1259	12.950	1.2550	0.05
MIROC5	2.2396	0.5792	4.9999	0.0961	0.4486	0.0100	0.1234	2.8327	1.1048	0.15
MIROC-ESM	0.6896	0.1877	2.0219	0.4933	0.2884	1.4103	0.9501	3.6729	1.1383	0.12
MIROC-ESM-CHEM	0.9997	-0.5891	1.1388	1.1193	0.0254	9.6999	0.3022	4.4868	1.1277	0.05
MPI-ESM-LR	1.7898	-0.0385	3.2976	0.2319	0.8504	1.1209	0.2792	2.1975	1.2154	0.33
MPI-ESM-MR	2.0752	-1.2640	1.4401	0.5752	0.0510	10.000	0.5349	8.2459	1.1122	0.06
MPI-ESM-P	1.3946	-0.4808	4.4931	0.0898	0.0389	10.000	0.2498	3.9468	1.2927	0.07
MRI-CGCM3	1.4610	0.2543	4.2439	0.1300	0.1760	5.9552	0.0071	2.4876	1.1478	0.05
NorESM1-M	1.3714	0.4972	1.404	0.4805	1.0000	3.0676	0.2752	2.5603	1.1744	0.11
NorESM1-ME	2.8281	0.6425	2.8026	0.1382	0.2966	10.000	0.0266	15.706	1.1203	0.08
Mean	1.3547	-0.7115	1.7022	0.3602	0.5515	9.9876	0.2469	4.2944	0.8823	0.05

Table 2. Glacier sea level component calibration results with parameter sets for the available CMIP5 models. Calibration parameters are introduced in section 2.6. GOF is given as weighted RSS divided by the number of calibrated model years (weight glacier SLE contribution [mm]: 1). The optimal set for the mean response of the calibration data is given at the bottom of the table.

Model	κ	ν	GOF
BCC-CSM1.1	0.0131	0.1551	51.88
CanESM2	0.0098	0.1742	27.22
CCSM4	0.0104	0.2743	6.935
CNRM-CM5	0.0101	0.2217	122.8
CSIRO-Mk3.6.0	0.0088	0.2963	120.1
GFDL-CM3	0.0125	0.1932	6.061
GISS-E2-R	0.0116	0.0955	11.81
HadGEM2-ES	0.0114	0.2961	50.19
IPSL-CM5A-LR	0.0091	0.2260	33.82
MIROC5	0.0126	0.1198	12.77
MIROC-ESM	0.0099	0.1402	23.91
MPI-ESM-LR	0.0079	0.4451	25.04
MRI-CGCM3	0.0081	0.1885	13.10
NorESM1-M	0.0106	0.1126	34.04
Mean	0.0106	0.0788	6.10

Table 3. Greenland SMB sea level component calibration results with optimal parameter sets for the available CMIP5 models. Calibration parameters are introduced in section 2.6. GOF is given as weighted RSS divided by the number of calibrated model years (weight Greenland SMB SLE contribution [mm]: 1). The optimal set for the mean response of the calibration data is given at the bottom of the table.

Model	υ	χ	φ	GOF
ACCESS1.0	0.2190	0.9748	3.2749	0.74
ACCESS1.3	0.2021	0.2490	1.2781	0.46
BCC-CSM1.1	0.0664	0.2398	2.3731	0.56
BNU-ESM	0.1290	0.0000	1.9068	0.89
CanESM2	0.0656	0.0000	2.2971	1.96
CCSM4	0.0186	0.0000	2.7122	1.17
CESM1-BGC	0.0618	0.0000	1.9517	1.06
CMCC-CM	0.0830	0.0000	1.9688	1.57
CNRM-CM5	0.1009	0.0000	1.8283	0.36
CSIRO-Mk3.6.0	0.1459	0.4702	1.8740	0.60
GFDL-CM3	0.3347	0.7326	2.2962	0.56
GFDL-ESM2M	0.1077	0.0000	2.0794	0.90
GISS-E2-R	0.1302	0.0000	1.9605	0.26
HadGEM2-CC	0.2308	0.9594	2.9988	0.27
HadGEM2-ES	0.1974	0.8354	2.2872	0.55
IPSL-CM5A-LR	0.1762	0.4514	1.8847	0.25
IPSL-CM5A-MR	0.0802	0.0000	2.0480	0.67
IPSL-CM5B-LR	0.0531	0.0000	2.4263	0.99
MIROC5	0.2168	0.0000	1.8440	1.11
MIROC-ESM-CHEM	0.1557	0.3454	2.1621	1.51
MIROC-ESM	0.1549	0.5188	2.3107	1.10
MPI-ESM-LR	0.0333	0.0000	2.6372	1.49
MRI-CGCM3	0.0645	0.0000	2.2958	0.59
NorESM1-M	0.0969	0.0000	2.0000	0.50
Mean	0.1148	0.0000	2.0169	0.47

Table 4. Greenland SID sea level component calibration results with optimal parameter sets for the low and high cases introduced by Nick et al. (2013). Calibration parameters are introduced in section 2.6. GOF is given as weighted RSS divided by the number of calibrated model years (weight Greenland SID SLE contribution [mm]: 1).

Case	ϱ	ϵ	GIS_{max}^{outlet} [mm]	GOF
low	9.062e-04	0.3891	35.98	0.81
high	7.933e-04	0.4722	53.63	1.62

Table 5. Antarctic SMB sea level component calibration results with optimal parameter sets for the CMIP3 models ECHAM5 and HadCM3. Calibration parameters are introduced in section 2.6. GOF is given as weighted RSS divided by the number of calibrated model years (weight Antarctic SMB SLE contribution [mm]: 1). The optimal set for the mean response of the calibration data is given at the bottom of the table.

Model	ξ	ρ	σ	GOF
ECHAM5	-0.11028	0.0000	1.2435	0.70
HadCM3	-0.13869	0.0000	1.3910	9.61
Mean	-0.12082	0.0000	1.5234	0.70

Table 6. 2081-2100 median values and 66% ranges for global SLR projections relative to 1986-2005 in meters, resolved by sea level components for the four RCP scenarios. Estimates are provided based on the CMIP5 consistent MAGICC setup. IPCC median projections and likely ranges are given as a reference.

2081-2100		RCP2.6	RCP4.5	RCP6.0	RCP8.5
Total	MAGICC	0.41 [0.32 to 0.51]	0.49 [0.41 to 0.60]	0.49 [0.40 to 0.62]	0.67 [0.55 to 0.83]
	IPCC	0.40 [0.26 to 0.55]	0.47 [0.32 to 0.63]	0.48 [0.33 to 0.63]	0.63 [0.45 to 0.82]
Thermal Expansion	MAGICC	0.12 [0.08 to 0.17]	0.16 [0.12 to 0.22]	0.17 [0.12 to 0.23]	0.26 [0.19 to 0.34]
	IPCC	0.14 [0.10 to 0.18]	0.19 [0.14 to 0.23]	0.19 [0.15 to 0.24]	0.27 [0.21 to 0.33]
Glaciers	MAGICC	0.11 [0.09 to 0.14]	0.13 [0.10 to 0.15]	0.13 [0.10 to 0.15]	0.15 [0.13 to 0.17]
	IPCC	0.10 [0.04 to 0.16]	0.12 [0.06 to 0.19]	0.12 [0.06 to 0.19]	0.16 [0.09 to 0.23]
Greenland SMB	MAGICC	0.03 [0.01 to 0.04]	0.03 [0.02 to 0.05]	0.03 [0.02 to 0.05]	0.06 [0.04 to 0.09]
	IPCC	0.03 [0.01 to 0.07]	0.04 [0.01 to 0.09]	0.04 [0.01 to 0.09]	0.07 [0.03 to 0.16]
Greenland SID	MAGICC	0.03 [0.03 to 0.04]	0.03 [0.03 to 0.04]	0.03 [0.03 to 0.04]	0.05 [0.04 to 0.06]
	IPCC	0.04 [0.01 to 0.06]	0.04 [0.01 to 0.06]	0.04 [0.01 to 0.06]	0.05 [0.02 to 0.07]
Antarctica SMB	MAGICC	-0.02 [-0.03 to -0.01]	-0.02 [-0.03 to 0.02]	-0.02 [-0.04 to -0.02]	-0.04 [-0.05 to -0.03]
	IPCC	-0.02 [-0.04 to -0.00]	-0.02 [-0.05 to -0.01]	-0.02 [-0.05 to -0.01]	-0.04 [-0.07 to -0.01]
Antarctica SID	MAGICC	0.07 [0.04 to 0.14]	0.08 [0.05 to 0.16]	0.08 [0.05 to 0.16]	0.11 [0.06 to 0.21]
	IPCC	0.07 [-0.01 to 0.16]	0.07 [-0.01 to 0.16]	0.07 [-0.01 to 0.16]	0.07 [-0.01 to 0.16]
Land water storage	MAGICC	0.06 [0.05 to 0.07]	0.06 [0.05 to 0.07]	0.06 [0.05 to 0.07]	0.06 [0.05 to 0.07]
	IPCC	0.04 [-0.01 to 0.09]	0.04 [-0.01 to 0.09]	0.04 [-0.01 to 0.09]	0.04 [-0.01 to 0.09]

Table 7. 2100 and 2300 median values as well as 66% ranges for total global SLR projections relative to 1986-2005 based on the MAGICC CMIP5 and MAGICC PROB experimental designs. IPCC median projections and likely ranges are given as a reference.

		2100	2300
RCP2.6	MAGICC CMIP5	0.45 [0.35 to 0.59]	-
	MAGICC PROB	0.48 [0.37 to 0.59]	1.01 [0.80 to 1.35]
	IPCC	0.44 [0.28 to 0.61]	-
RCP4.5	MAGICC CMIP5	0.55 [0.45 to 0.67]	-
	MAGICC PROB	0.61 [0.47 to 0.74]	1.75 [1.29 to 2.30]
	IPCC	0.53 [0.36 to 0.71]	-
RCP6.0	MAGICC CMIP5	0.56 [0.46 to 0.71]	-
	MAGICC PROB	0.65 [0.51 to 0.80]	2.37 [1.72 to 3.20]
	IPCC	0.55 [0.38 to 0.73]	-
RCP8.5	MAGICC CMIP5	0.79 [0.65 to 0.97]	-
	MAGICC PROB	0.88 [0.68 to 1.08]	4.73 [3.41 to 6.83]
	IPCC	0.74 [0.52 to 0.98]	-

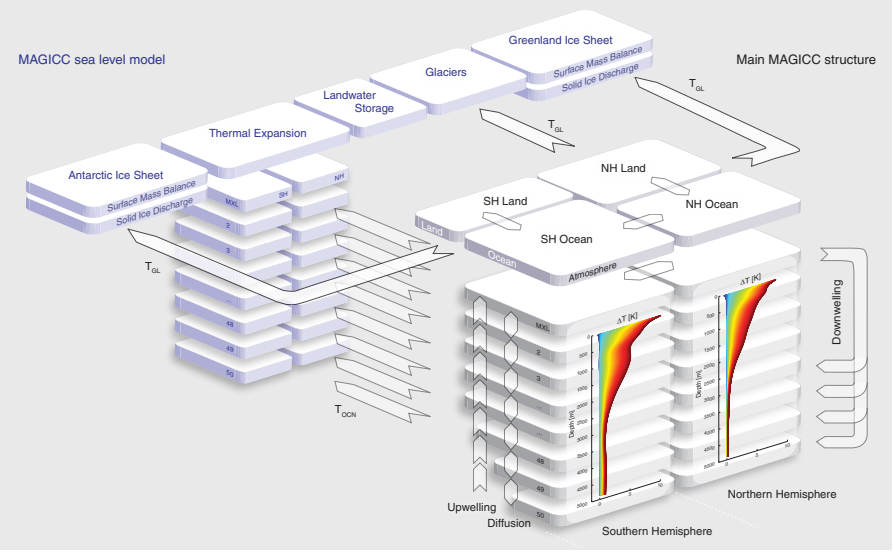

Figure 1. Schematic of the MAGICC sea level model structure and the driving MAGICC hemispheric upwelling-diffusion energy balance core. Heat is transported through the oceans by downwelling and corresponding layer entrainment, upwelling, diffusion, and the exchange between the hemispheres. Ocean mixed layer is denoted MXL, depth-dependent ocean areas are shown by smaller ocean layers towards the ocean bottom. Illustrative potential ocean temperature warming profiles that feed into the layer-dependent thermal expansion module are sketched for both hemispheres. Ocean and air temperature fluxes (T_{OCN},T_{GL}) relevant for the sea level model as well as other major energy fluxes are shown as arrows. Figure adapted from Meinshausen et al. (2011a).

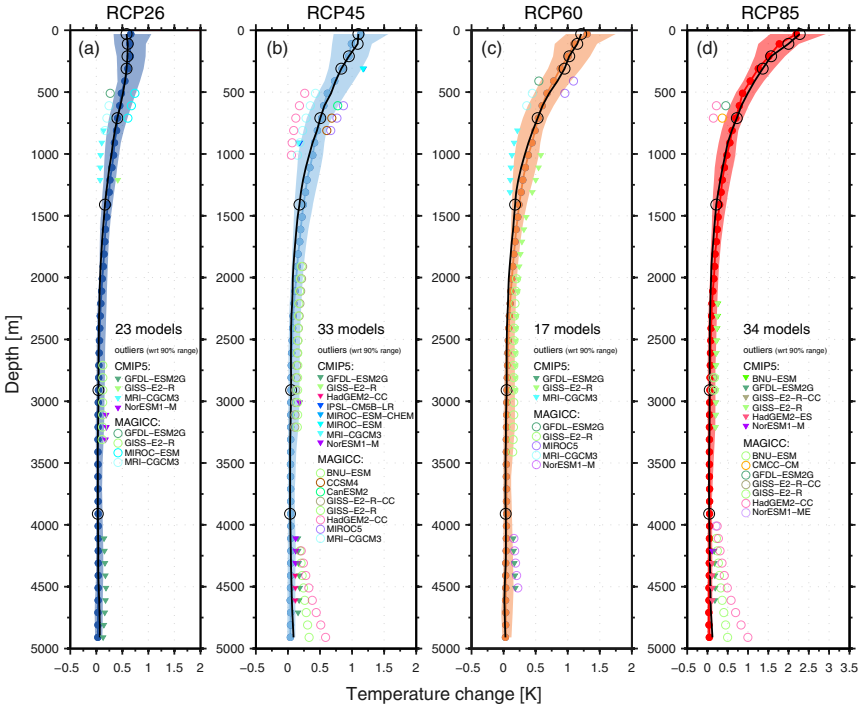

Figure 2. Potential ocean temperature depth profiles for MAGICC and reference CMIP5 warming under RCP2.6, RCP4.5, RCP6.0 and RCP8.5 scenarios, 2081-2100 anomalies with respect to 1986-2005. Interpolated CMIP5 90% model ranges and corresponding median profiles are shown in colors, with circles indicating the individual MAGICC ocean layers. MAGICC median ocean warming profiles given as black lines with open circles indicating selected layers for ocean calibration. Model Outliers not covered by the respective 90% ranges are shown for both CMIP5 reference data and MAGICC calibration results. Potential ocean temperature residuals of the calibration are provided for every MAGICC ocean layer in Figure A.1.

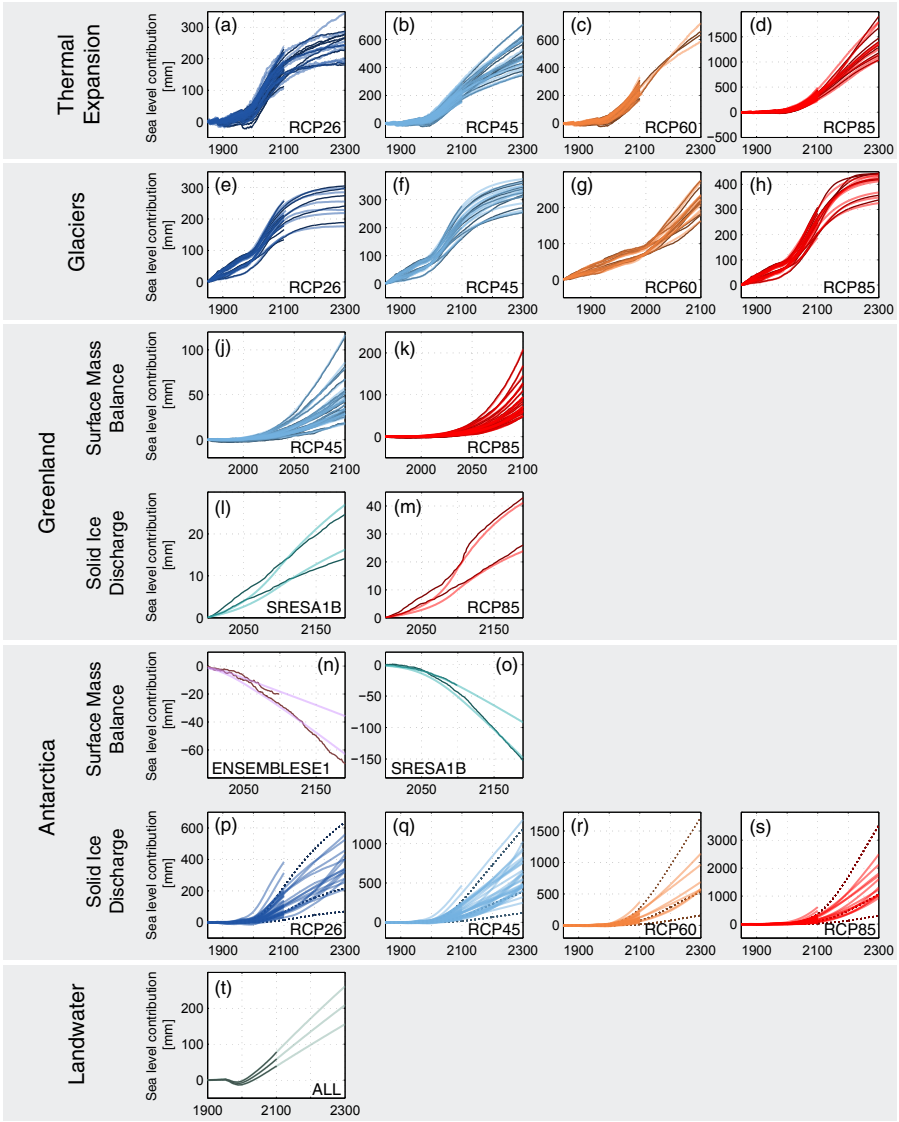

Figure 3. MAGICC sea level model calibration results for thermal expansion (a-d), global glaciers (e-h), Greenland surface mass balance (j-k) and solid ice discharge (l-m), Antarctic surface mass balance (n-o) and solid ice discharge (p-s), as well as land water (t). The panels show scenario-specific calibrated MAGICC sea level responses as coloured lines, with underlying reference data as thin dark lines. Antarctic solid ice discharge reference 90% range plus corresponding median are provided as thin dashed lines. Climate-independent land water projections are identical to the reference data until 2100 (see Section 2.5). Please note that x- and y-axis ranges differ for individual panels.

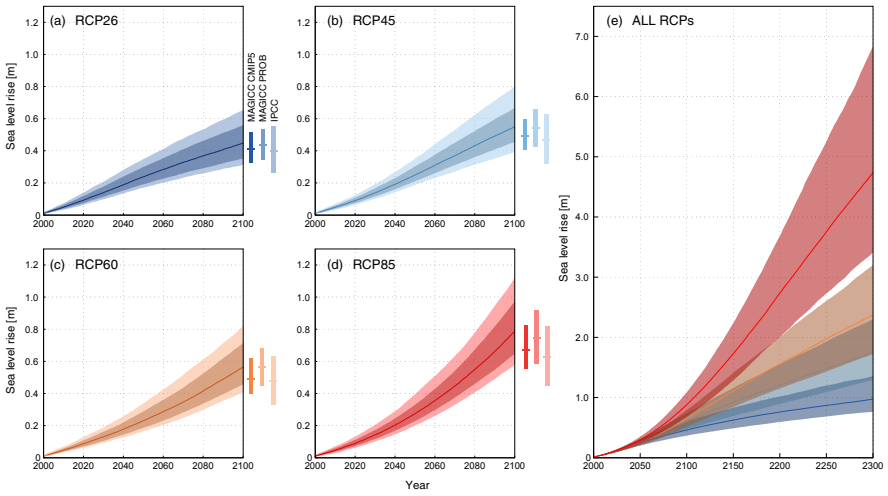

Figure 4. Global sea level projections until 2100 based on CMIP5 constrained MAGICC runs as anomalies relative to 1986-2005 in panels (a) to (d). 90% ensemble range in light colors, 66% ensemble range in darker colors, median as solid line. 2081-2100 anomalies with respect to 1986-2005 as vertical bars for CMIP5 constrained MAGICC setup (MAGICC CMIP5), historically-constrained probabilistic MAGICC setup (MAGICC PROB), and IPCC reference projections. 2300 sea level projections in panel (e) are showing 66% ranges for all RCP extensions based on MAGICC PROB; median estimates as solid lines.

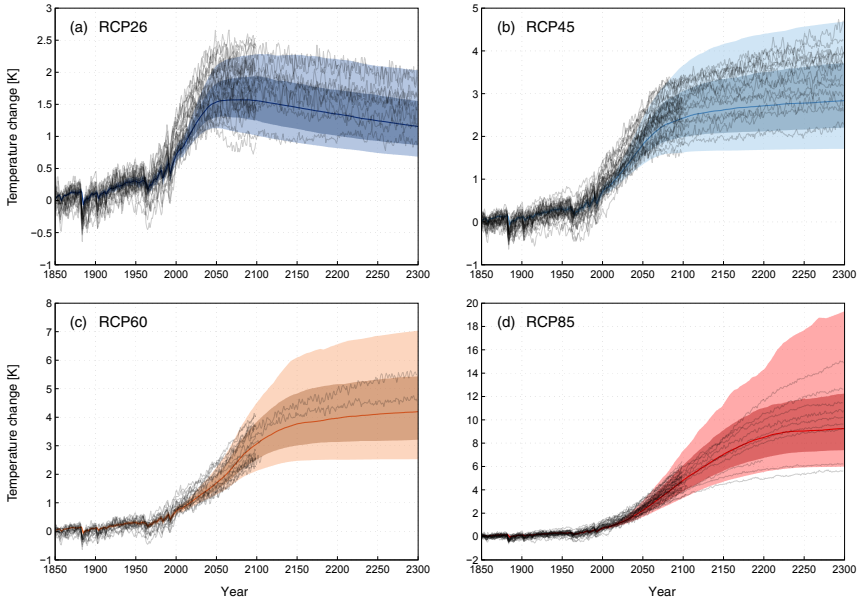

Figure 5. Global mean *tas* projections until 2300 for all RCP extensions based on the historically-constrained probabilistic MAGICC setup; 90% ensemble range in light colors, 66% ensemble range in darker colors, medians as solid lines. Available global CMIP5 *tas* reference time series are shown as thin black lines. All temperature projections are given relative to 1850.

Appendix A:

Additional information on MAGICC sea level model calibration parameters, MAGICC ocean model calibration results, MAGICC SLR hindcast quality, and component-wise MAGICC SLR projections for 1900-2300.

Table A.1. List of variables and free parameters used for the individual MAGICC sea level component calibrations.

Climate variables	Unit	Description
tas	K	surface air temperature
thetao	K	potential ocean temperature
zostoga	mm	thermal expansion
MAGICC ocean paramters		
K_z	$\frac{cm^2}{s}$	vertical thermal diffusivity
$\frac{dK_{z_{top}}}{dT}$	$\frac{cm^2}{sK}$	sensitivity to global mean *tas* at the mixed layer boundary
η	K	sea-ice adjustment offset
γ	$\frac{1}{K}$	sea-ice adjustment factor
w_0	$\frac{m}{yr}$	initial upwelling velocity
β		ratio of changes in temperature of entraining waters to polar sinking waters
$\frac{\Delta w_t}{w_t}$		ratio of variable to fixed upwelling for every time step
T_{w_t}	K	threshold temperatures for constant upwelling rates
ϕ		global thermal expansion scaling
Glacier parameters		
κ	$\frac{1}{K}$	glacier sensitivity
ν		temperature sensitivity exponent
Greenland SMB parameters		
υ	$\frac{mm}{K}$	temperature sensitivity
χ		relative magnitude of linear and non-linear terms
φ		temperature sensitivity exponent
Greenland SID parameters		
ϱ		discharge sensitivity
ϵ	$\frac{1}{K}$	temperature sensitivity
GIS_{max}^{outlet}	mm	maximum Greenland outlet glacier volume
Antarctic SMB parameters		
ξ	$\frac{mm}{K}$	temperature sensitivity
ρ		relative magnitude of linear and non-linear terms
σ		temperature sensitivity exponent

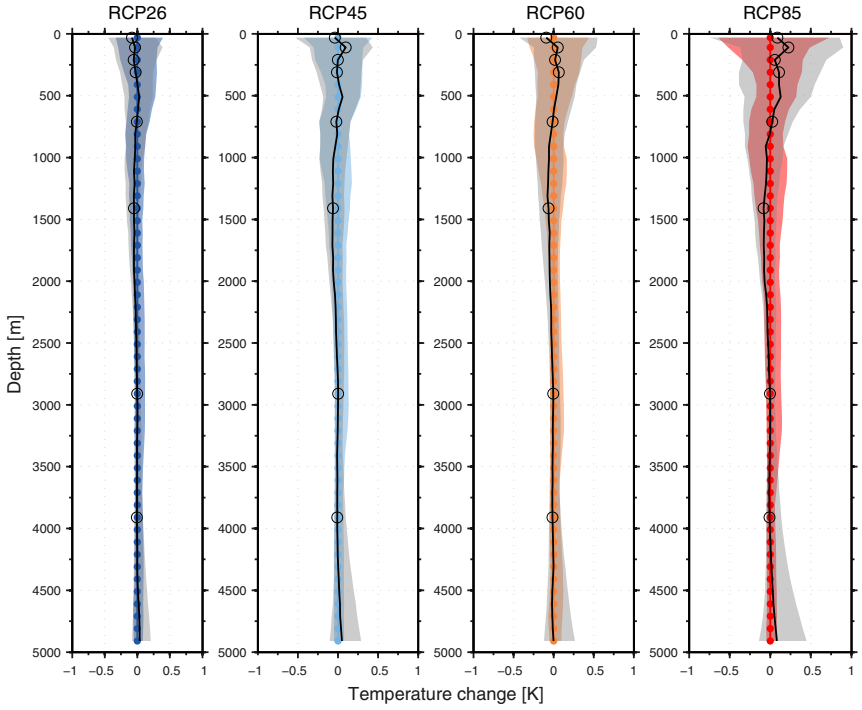

Figure A.1. Potential ocean temperature residuals for calibrated MAGICC and reference CMIP5 ocean warming under RCP2.6, RCP4.5, RCP6.0 and RCP8.5 scenarios. Residuals are given with respect to the median CMIP5 2081-2100 to 1986-2005 anomalies for every MAGICC ocean layer. CMIP5 reference median and 90% range are shown in color, with circles indicating the individual MAGICC ocean layers. Calibrated MAGICC 90% model range and median residuals are provided as grey shadings and black lines with open circles indicating the selected layers for the ocean calibration.

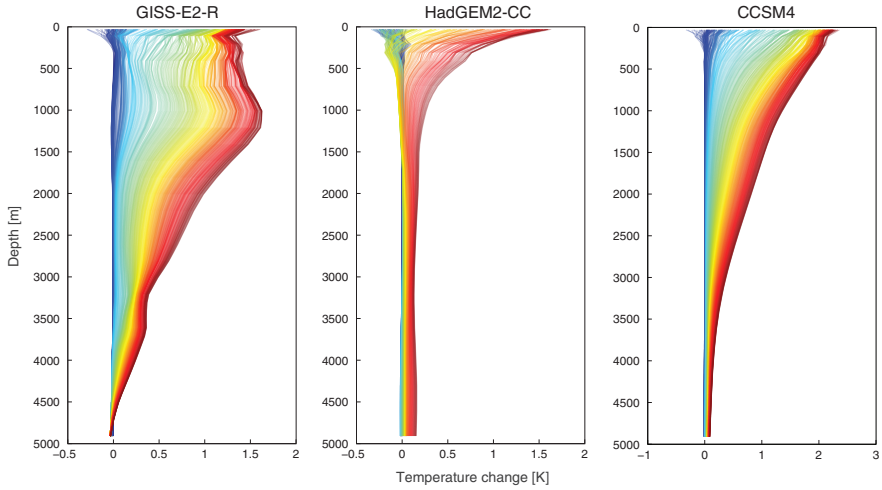

Figure A.2. Annual RCP4.5 ocean warming anomalies for the CMIP5 models GISS-E2-R (1850-2300), HadGEM2-CC (1850-2100), and CCSM (1850-2300), relative to 1850 and globally averaged. Annual potentential ocean temperature anomaly profiles are shown as dark blue in 1850 via green and yellow to red for the last year of the reference data.

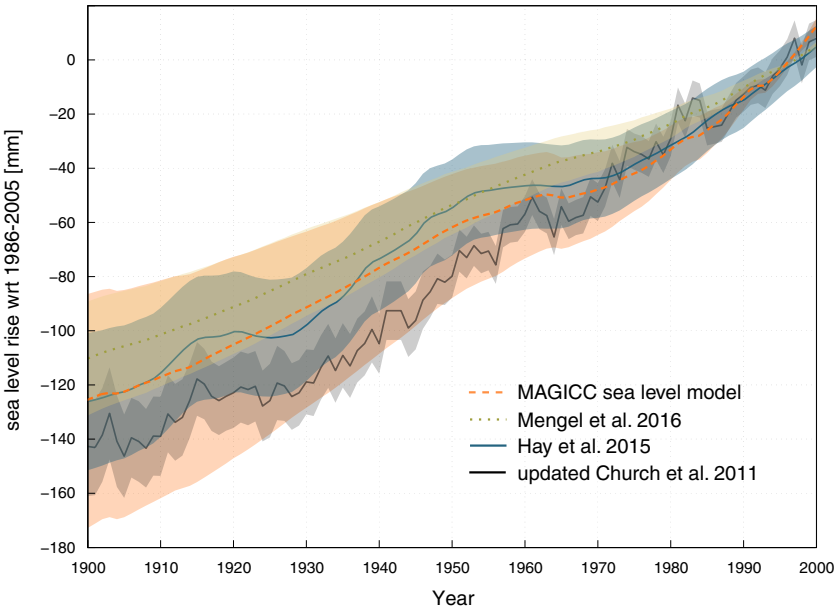

Figure A.3. Historical modelled and observed SLR from 1900 to 2000, relative to the 1986-2005 mean. Median and 90% uncertainty ranges are shown for the MAGICC hindcast (orange) and results from Mengel et al. (2016) (khaki), with observed sea level time series and respective uncertainties based on Hay et al. (2015) (blue) and the updated Church et al. (2011) datasets (grey).

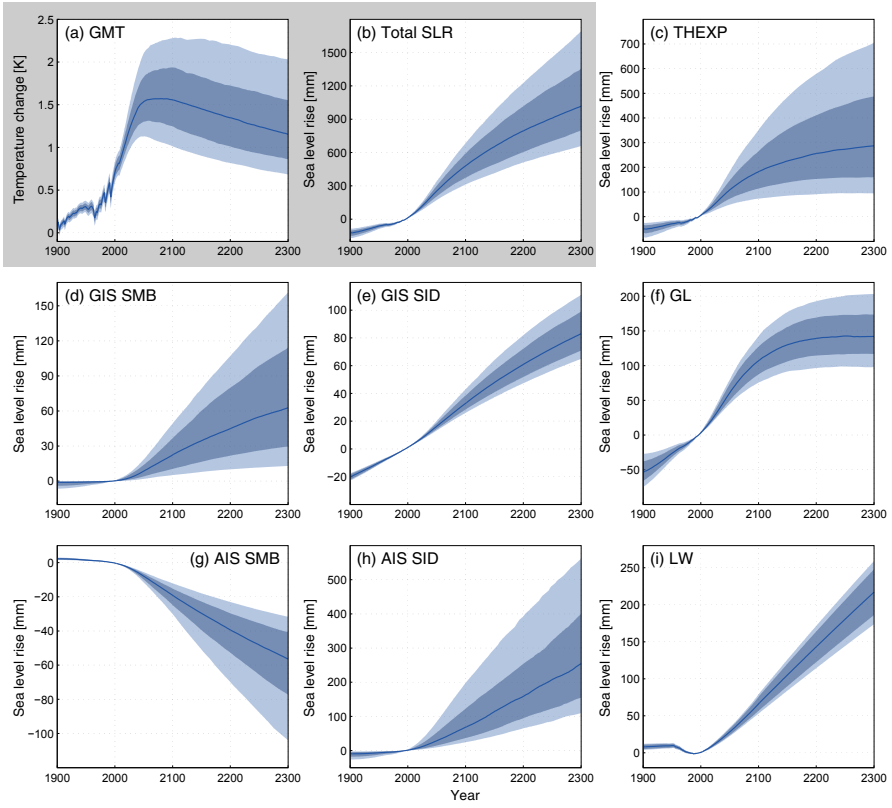

Figure A.4. 1900-2300 SLR projections resolved by the indiviual MAGICC sea level components for RCP2.6 in mm. We show median estimates, 66% ranges in darker shading, and 90% ranges in lighter shading for MAGICC GMT output relative to pre-industrial in panel (a), total SLR in panel (b), thermal expansion (THEXP) in panel (c), Greenland Ice Sheet (GIS) SMB and SID in panels (d) and (e), global glacier (GL) in panel (f), Antarctic ice sheet (AIS) SMB and SID in panels (g) and (h), and land water LW in panel (i). All sea level contributions are provided relative to 1986-2005.

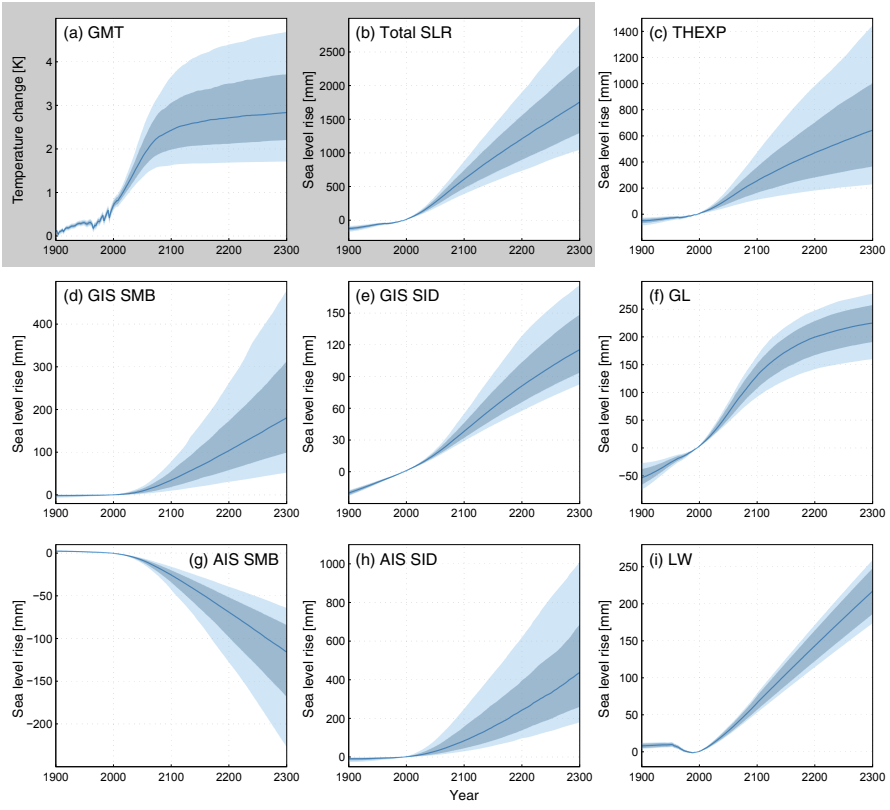

Figure A.5. 1900-2300 SLR projections resolved by the indiviual MAGICC sea level components for RCP4.5 in mm. We show median estimates, 66% ranges in darker shading, and 90% ranges in lighter shading for MAGICC GMT output relative to pre-industrial in panel (a), total SLR in panel (b), thermal expansion (THEXP) in panel (c), Greenland Ice Sheet (GIS) SMB and SID in panels (d) and (e), global glacier (GL) in panel (f), Antarctic ice sheet (AIS) SMB and SID in panels (g) and (h), and land water LW in panel (i). All sea level contributions are provided relative to 1986-2005.

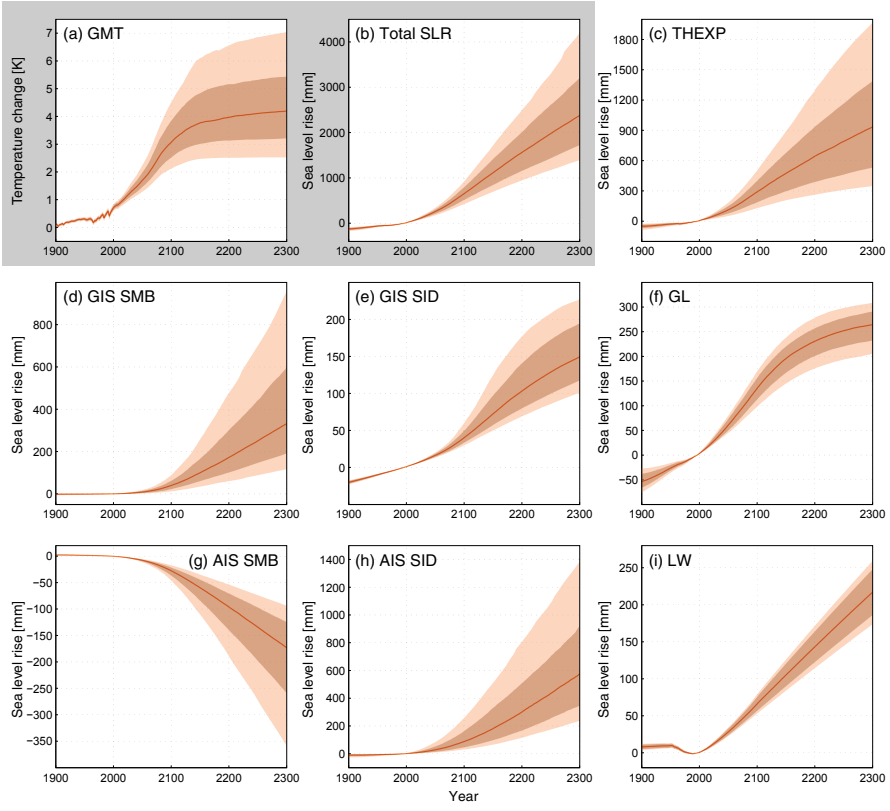

Figure A.6. 1900-2300 SLR projections resolved by the indiviual MAGICC sea level components for RCP6.0 in mm. We show median estimates, 66% ranges in darker shading, and 90% ranges in lighter shading for MAGICC GMT output relative to pre-industrial in panel (a), total SLR in panel (b), thermal expansion (THEXP) in panel (c), Greenland Ice Sheet (GIS) SMB and SID in panels (d) and (e), global glacier (GL) in panel (f), Antarctic ice sheet (AIS) SMB and SID in panels (g) and (h), and land water LW in panel (i). All sea level contributions are provided relative to 1986-2005.

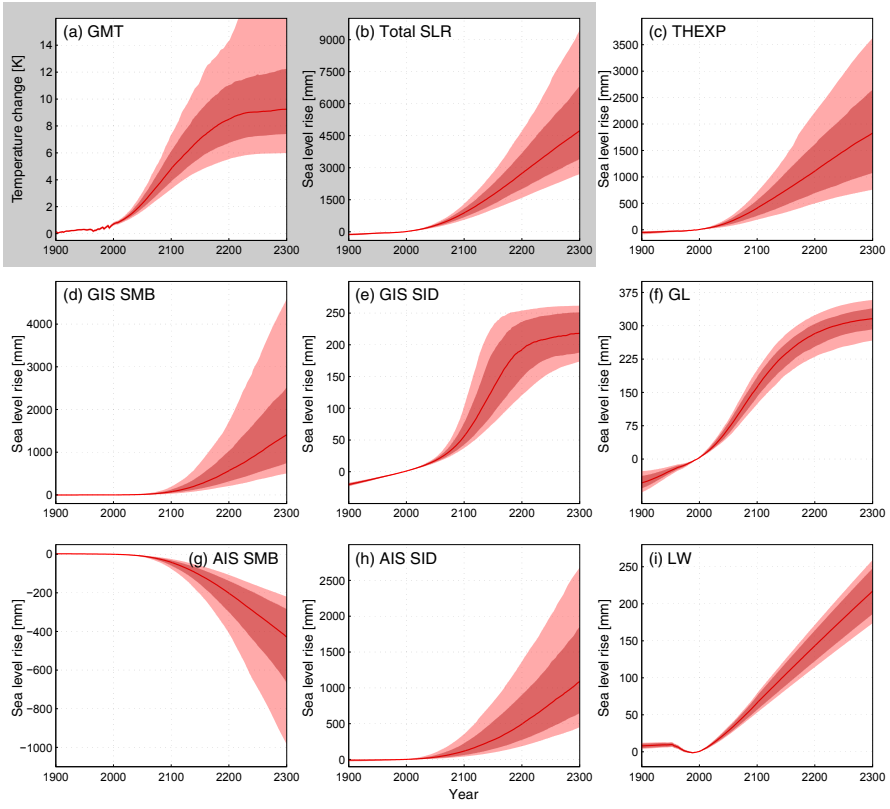

Figure A.7. 1900-2300 SLR projections resolved by the indiviual MAGICC sea level components for RCP8.5 in mm. We show median estimates, 66% ranges in darker shading, and 90% ranges in lighter shading for MAGICC GMT output relative to pre-industrial in panel (a), total SLR in panel (b), thermal expansion (THEXP) in panel (c), Greenland Ice Sheet (GIS) SMB and SID in panels (d) and (e), global glacier (GL) in panel (f), Antarctic ice sheet (AIS) SMB and SID in panels (g) and (h), and land water LW in panel (i). All sea level contributions are provided relative to 1986-2005.